npj | Computational Materials

www.nature.com/npjcompumats

REVIEW ARTICLE OPEN

On the tuning of electrical and thermal transport in thermoelectrics: an integrated theory–experiment perspective

Jiong Yang[1], Lili Xi[2], Wujie Qiu[2,3], Lihua Wu[1], Xun Shi[2], Lidong Chen[2], Jihui Yang[4], Wenqing Zhang[1,2], Ctirad Uher[5] and David J Singh[6]

During the last two decades, we have witnessed great progress in research on thermoelectrics. There are two primary focuses. One is the fundamental understanding of electrical and thermal transport, enabled by the interplay of theory and experiment; the other is the substantial enhancement of the performance of various thermoelectric materials, through synergistic optimisation of those intercorrelated transport parameters. Here we review some of the successful strategies for tuning electrical and thermal transport. For electrical transport, we start from the classical but still very active strategy of tuning band degeneracy (or band convergence), then discuss the engineering of carrier scattering, and finally address the concept of conduction channels and conductive networks that emerge in complex thermoelectric materials. For thermal transport, we summarise the approaches for studying thermal transport based on phonon–phonon interactions valid for conventional solids, as well as some quantitative efforts for nanostructures. We also discuss the thermal transport in complex materials with chemical-bond hierarchy, in which a portion of the atoms (or subunits) are weakly bonded to the rest of the structure, leading to an intrinsic manifestation of part-crystalline part-liquid state at elevated temperatures. In this review, we provide a summary of achievements made in recent studies of thermoelectric transport properties, and demonstrate how they have led to improvements in thermoelectric performance by the integration of modern theory and experiment, and point out some challenges and possible directions.

npj Computational Materials (2016) **2,** 15015; doi:10.1038/npjcompumats.2015.15; published online 26 February 2016

INTRODUCTION

Thermoelectric (TE) materials are materials that can generate useful electric potentials when subjected to a temperature gradient (known as the Seebeck effect). Conversely, they also transfer heat against the temperature gradient when a current is driven against this potential (known as the Peltier effect). They are promising energy materials with many applications, such as waste heat harvesting, radioisotope TE power generation, and solid state Peltier refrigeration, all of which are driving growing research interest. A key challenge is to improve the TE properties in order to obtain more efficient energy conversion and in turn enable new practical applications. Good TE materials must have excellent electrical transport properties, measured by the TE power factor ($=S^2\sigma$, where S is the Seebeck coefficient and σ is the electrical conductivity), and also a very low thermal conductivity κ (composed of the electronic contribution κ_e, the lattice contribution κ_L, and the bipolar contribution κ_{bi}). Combining the two aspects gives us the dimensionless figure of merit ZT,

$$\mathrm{ZT} = \frac{S^2\sigma T}{\kappa}, \qquad (1)$$

where T is the absolute temperature. ZT is the key parameter that characterises the energy conversion efficiency that is possible using a given TE material.

Optimisation of the TE performance of materials has proved to be difficult since the three transport parameters, i.e., S, σ and κ, are intercorrelated in a way that works against the occurrence of high ZT. For instance, increasing the Seebeck coefficient S usually means lowering the electrical conductivity σ, and vice versa; the electronic thermal conductivity κ_e also relates with the electrical conductivity σ via the Wiedemann–Franz law $\kappa_e = L\sigma T$ (L is the Lorenz number). The correlations among the parameters were studied in the early 1960s, and the best TE materials were identified to be narrow band gap semiconductors with some amount of doping (the optimal carrier concentration usually ranging from 10^{19} to 10^{21} cm^{-3}), leading to the first step forward in the TE research.[1,2] The carrier mobility μ and the band effective mass m^* present another important consideration. High m^* is beneficial to S; however, under single parabolic band (SPB) model and acoustic phonon scattering mechanism, high m^* reduces μ. Novel band engineering is necessary to break up this relationship. Several excellent reviews have discussed interrelations in the electrical transport and outlined possible solutions.[3,4] The lattice thermal conductivity κ_L is more or less independent of the electronic parameters. However, the traditional ways of achieving low κ_Ls, such as forming solid solutions or making composite structures, typically have a detrimental effect on the carrier mobility μ. A judicious choice of the grain size between the critical lengths for the electrical and the heat transport, which could preferentially scatter phonons, and/or introducing appropriate structural units that tend to optimise the two types of transport separately, were regarded as best solutions for the optimisation of μ/κ_L. Before 1990s, the exact recipes how to break the above-mentioned dilemmas of optimisation were either unclear, or hard

[1]Materials Genome Institute, Shanghai University, Shanghai, China; [2]State Key Laboratory of High Performance Ceramics and Superfine Microstructure, Shanghai Institute of Ceramics, Chinese Academy of Sciences, Shanghai, China; [3]Department of Physics, East China Normal University, Shanghai, China; [4]Material Science and Engineering Department, University of Washington, Seattle, WA, USA; [5]Department of Physics, University of Michigan, Ann Arbor, MI, USA and [6]Department of Physics and Astronomy, University of Missouri, Columbia, MO, USA.
Correspondence: L Chen (cld@mail.sic.ac.cn) or J Yang (jihuiy@uw.edu) or W Zhang (wqzhang@mail.sic.ac.cn)
Received 14 October 2015; revised 10 December 2015; accepted 10 December 2015

to achieve experimentally and the best values of ZT stagnated near unity for about 30 years.

Some 20 years ago, two big ideas shed light on new directions in the field of thermoelectricity. Hicks and Dresselhaus proposed to utilise quantum well structures, aiming to enhance the power factor by altering the electronic density of states (DOS) in lower dimensions.[5,6] Although the quantum well structures are hard to fabricate even today, their main features can be imported into the realm of bulk materials by the state-of-the-art band engineering strategies. Moreover, lower dimensional structures with numerous interfaces, very effectively scatter the heat-carrying phonons and thus significantly reduce the lattice thermal conductivity.[3,7,8] The other important idea was the 'Phonon Glass Electron Crystal' (PGEC) paradigm, proposed by Slack.[9] It describes an ideal architecture of new TE materials with potentially independent electrical and thermal transport networks. The concept gave rise to intense studies on new complex compounds (e.g., filled skutterudites and clathrates) with atomic-level heterogeneity, different from the traditional binary TE compounds. Inspired by these two ideas, the field of thermoelectricity received a second major impulse in the late 1990s, which continues unabated till today.

The first major advance some half a century ago was theoretically underpinned by the classical SPB band model for electrical transport optimisation and by heavy elements, solid solutions and so on, for thermal transport reduction. The second and the more recent impetus mentioned above is based on new concepts, such as the role of a nanostructure, band (or scattering) engineering and complex structures. It is obvious that understanding the microscopic phenomena is critical, and this presents new challenges for the experimentalists. Take the band engineering as an example that relies on accurate information regarding the band structure and its momentum-dependence. The regular experimental characterisation of the transport parameters, such as the carrier concentrations and the effective masses, is usually extracted based on analytic band models, particularly the well-accepted SPB model. The main characters of the band of a material are reflected by the effective mass in an averaged way. Being simple and analytically clear, the SPB approach is considered to be very useful in understanding the general trend of transport properties and their dependence on carrier concentration, such as those reflected in the Pisarenko curves. Efforts beyond the SPB model by considering multiple bands and even non-parabola makes those expressions very complex and are only taken to explain the experimental data for very specific systems. The direct techniques of determining the band structure in experiments, e.g., angle-resolved photoemission spectroscopy, are seldom used in TEs due to some technical limitations, e.g., the requirements of single-crystal sample, extremely low temperatures and sensitivity to the surface contamination and so on.[10] Effective way of band structure characterisation for complex TE materials is still in a developing stage. Even if such measurements were available, it would still be difficult to touch upon more fundamental information concerning the nature of chemical bonds in order to reliably determine any band variation.

Theoretical work, including modelling and *ab initio*-based calculations, naturally span length scales from sub-angstrom to tens of nanometer and provide the bottom–up information. Band structure calculations can help to rationalise the band engineering, in a more direct way.[11] Additional information the theoretical work can offer includes the total energy, electronic and phonon dispersions, as well as atomic movement in a larger scale simulation. Although theoretical calculations cannot fully represent the experimental reality owing to some approximations and technical difficulties (e.g., the neglect of thermal motion in standard density functional calculations, the difficulties on the treatment of defects, as well as carrier scatterings), they still become a complementary tool to experimental techniques in modern research on thermoelectrics. Over the years, integrated theory–experiment studies have greatly improved understanding of TE transport and at the same time have greatly speeded up and advanced the optimisation of materials leading to enhancements in ZT values. The increasing numbers of integrated research efforts bode very well for the future success of TE research.

It has been exactly 20 years since Slack proposed the PGEC concept and since that time one has witnessed many important theoretical contributions providing new ideas that have advanced the field of thermoelectricity in a fundamental way. It is necessary then to provide a bird's eye view of the theoretical understanding and ideas in TEs and its integration with experiment. This is the main aim of this paper. We basically focus on the electrical and thermal transport processes. In the electrical transport ('Electrical Transport in Thermoelectrics'), we start from engineering both the band and scattering phenomena, as well as describing the concept of conductive networks emerging in complex TE materials. For the thermal transport ('Thermal Transport in Thermoelectrics'), we summarise the traditional approaches for κ_L reduction in conventional solids, including strong phonon-phonon interactions (PPIs) and the influence of nanostructures. Then, we review the work on thermal transport in complex materials possessing chemical-bond hierarchy. A few TE materials with synergistically optimised electrical and thermal transports will be briefly discussed in 'Synergistic Optimisation for High ZTs'.

ELECTRICAL TRANSPORT IN THERMOELECTRICS

The electrical transport properties are determined by the electronic structures of the materials and various carrier-scattering processes. The commonly used formulas based on Boltzmann transport theory for the electrical conductivity and the Seebeck coefficient are (tensor notions are omitted),[12]

$$\sigma(T) = \frac{1}{\Omega}\int \overline{\sigma}(\varepsilon)\left[-\frac{\partial f_0(T,\varepsilon)}{\partial \varepsilon}\right]d\varepsilon, \tag{2}$$

$$S(T) = \frac{1}{eT\Omega\sigma}\int \overline{\sigma}(\varepsilon)(\varepsilon-\varepsilon_F)\left[-\frac{\partial f_0(T,\varepsilon)}{\partial \varepsilon}\right]d\varepsilon. \tag{3}$$

Here ε_F, Ω, f_0, e are the Fermi level, the volume of the cell calculated, the Fermi–Dirac distribution, and the electron charge, respectively. The essential part in equations (2) and (3) is the transport distribution function (TDF),

$$\overline{\sigma}(\varepsilon) = \frac{e^2}{N}\sum_{i,\mathbf{k}}\tau_{i,\mathbf{k}}\mathbf{v}_{i,\mathbf{k}}^2\frac{\delta(\varepsilon-\varepsilon_{i,\mathbf{k}})}{d\varepsilon}, \tag{4}$$

where N and i are the number of $\mathbf{k}$ points sampling and band index, respectively. $\mathbf{v}$ is the group velocity and τ is the relaxation time. The latter can be approximately expressed in the energy dependent form,

$$\tau = \tau_0\varepsilon^r, \tag{5}$$

where τ_0 and r are constants for a given scattering mechanism.

The 'effective' electronic structures responsible for the electrical transport are within a narrow energy span determined by $-\partial f_0/\partial\varepsilon$. The term $(\varepsilon-\varepsilon_F)$, appearing in the numerator of the Seebeck coefficient (equation (3)), is of particular importance. It means the TDF on different sides of the Fermi level has an opposite contribution to the Seebeck coefficient. Rapidly changing TDF around the Fermi level is then favourable for a large Seebeck coefficient, which could be achieved by the manipulation of either DOS $N(\varepsilon)$ or relaxation time τ around ε_F, as shown in Figure 1. These manipulations can also be rationalised by the Mott relation,

$$S = \frac{\pi^2}{3}\frac{k_B^2}{e}T\left\{\frac{1}{n}\frac{dn(\varepsilon)}{d\varepsilon}+\frac{1}{\mu}\frac{d\mu(\varepsilon)}{d\mu}\right\}_{\varepsilon=\varepsilon_F}, \tag{6}$$

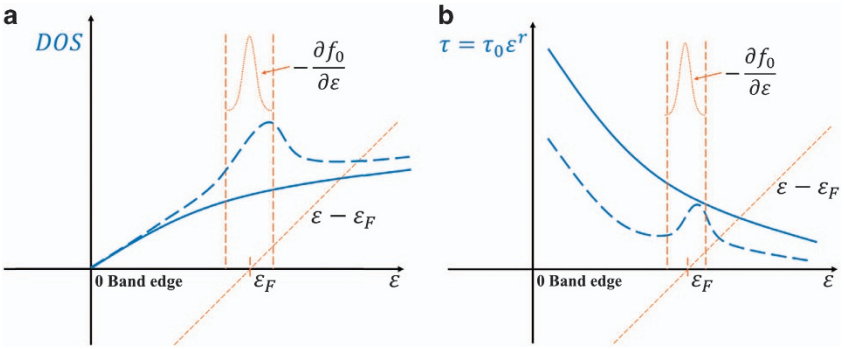

Figure 1. Schematic plots for (**a**) band engineering and (**b**) scattering engineering, with the blue dashed curves representing the manipulated cases.

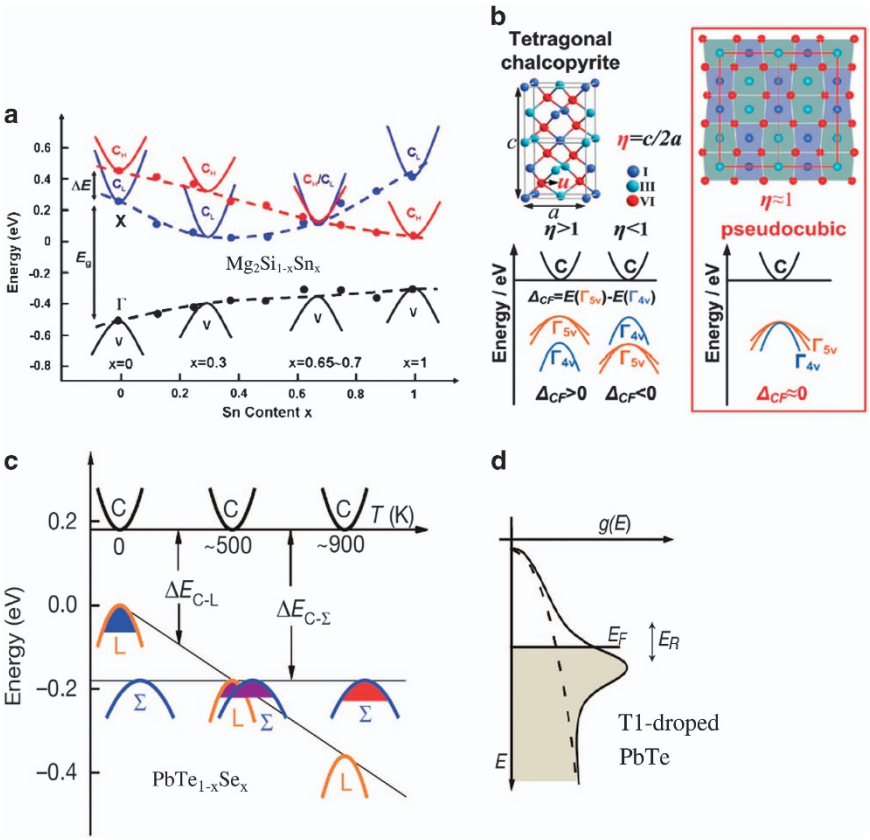

Figure 2. Several reported strategies for band engineering. (**a**) Proper solid solution composition in $Mg_2Si_{1-x}Sn_x$;[14] (**b**) The pseudocubic structure in tetragonal chalcopyrite compounds;[17] (**c**) temperature induced band order evolution in $PbTe_{1-x}Se_x$;[22] (**d**) Enhanced DOS in PbTe by the resonant states induced by the doping of Tl.[38]

where k_B is the Boltzmann constant. We can see that the enhanced energy dependence of the carrier concentration n (can be from a local increase in $N(\varepsilon)$) and the mobility μ is beneficial for the Seebeck coefficient. These are the bases for band and scattering engineering, which will be detailed in 'Band engineering for enhanced power factors' and 'Manipulation of carrier scattering', respectively.

In 'Carrier conductive network', we will review the concept of 'conductive network' in complex compounds. This concept applies to those multinary compounds where only part of the components is responsible for the electrical transport, which is distinct from the traditional binary TE materials. This will be elucidated in detail by several theory–experiment efforts in certain model systems, and some well-accepted qualitative features have been concluded for conductive networks.

Band engineering for enhanced power factors

The beneficial effects of a large-band degeneracy have long been recognised, as discussed by Goldsmid.[1] The energy-degenerate band edges (or band convergence in another words[13]) instead of energy separated ones can enhance the energy dependence of DOS at the Fermi level (Figure 1a), favourable for achieving large Seebeck coefficients for a fixed carrier density. On the other hand, the band shape for each energy pocket is unchanged, and thus the group velocities will not be largely altered. The twofold influence is the basis for enhancing the power factor of many TE materials by a large-band degeneracy. Several strategies for band engineering will be reviewed in this subsection.

Solid solutions between compounds with different band orders can serve as an effective strategy to achieve band convergence at

proper compositions, as shown in Mg_2X (X = Si and Sn) solid solution. The conduction band of Mg_2Si and Mg_2Sn shows a typical dual band structure (one light and one heavy band) with an inverted band order in the two compounds. *Ab initio* calculations done by Liu *et al.*[14] revealed that the position of the band edges varies with the composition as shown in Figure 2a, and the band edges of the light and heavy conduction bands coincide at the composition $Mg_2Si_{0.35}Sn_{0.65}$. The enhanced Seebeck coefficient and the unaffected electrical conductivity resulted in a significantly higher power factor over the parent compounds. The result was reproduced in the analytical work by Bahk *et al.*[15] As the usage of solid solutions is very common in TEs for the purpose of reducing κ_L, it is useful then to examine the band structure of the parent compounds and their solid solutions for the possibility of realising band convergence.

Tetragonal chalcopyrite semiconductors demonstrate another way how to achieve large band degeneracy by tuning the structural parameters. The valence band structure of binary cubic zinc-blende compounds consists of degenerate Γ_{5V} and Γ_{4V} bands.[16] After the cation cross-substitution into ternary or quaternary compositions with the tetragonal structure, the crystal-field splitting $\Delta_{CF} = \Gamma_{5V} - \Gamma_{4V}$ and a non-unity structural parameter $\eta = c/2a$ are observed (Figure 2b). By performing systematic calculations of transport properties, Zhang *et al.*[17] revealed a direct link between Δ_{CF} and η in ternary tetragonal chalcogenides, with $\eta \approx 1$ (pseudocubic structure) resulting in converged bands and enhanced power factors. The simple unity-η rule is useful for the screening of new candidates of tetragonal chalcopyrite semiconductors. It also suggests a direction of optimisation in these compounds by altering the η towards unity, which can be achieved through doping, composition tuning and solid solutions between compounds with $\eta > 1$ and $\eta < 1$, as shown in the experimental efforts in ternary and quaternary chalcogenides.[17,18]

In the compounds with multiple bands, the different band evolution with temperature may cause a crossing of band extrema at some point, together with enhanced transport properties. The temperature-induced band convergence has only been studied in PbTe and the related rock-salt IV–VI compounds (Figure 2c). These compounds possess non-parabolic edge states with the second or even the third energy pocket close to band edges, as revealed by Singh[19] and Chen *et al.*[20] The pockets, denoted as L, Σ and so on, have different temperature dependence, leading to the variations of both band gap[21] and the energy difference between pockets $\Delta E (= E_L - E_\Sigma)$ at finite temperatures.[22] The theoretical studies based on quasiharmonic approximation[23,24] show that the band evolution cannot be fully captured by the temperature-induced volume change. Using *ab initio* molecular dynamics (AIMD) and taking snapshots of structures for band calculations, Kim *et al.*[25] found that the L and Σ pockets converged at 450 K. The results of Gibbs *et al.*[26] further supported to the twofold contribution (lattice expansion and atomic displacement) to the L–Σ convergence, with the converged temperature was 700 K for PbTe. Generally speaking, the mechanism of temperature-induced band convergence is at the stage of rationalisation and more efforts are needed to get a better understanding of the phenomenon.

Defects, including vacancies, antisites, interstitials and elemental doping, can have a strong influence on both the electronic structure and charge-carrier scattering. From the band engineering point of view, defects offer another strategy to achieve band convergence by altering the bands. Explicitly, there are at least two types of band alterations by the defects: (i) altering relative band positions of the matrix (type-I) and (ii) introducing the so-called resonant levels via defect–host interactions (type-II). Numerous experiments[27–32] with IV–VI compounds have suggested that the tuning of the relative positions of different pockets by doping on the IV-site (type-I alterations). Some of the beneficial dopants were verified by *ab initio* band structure calculations, without looking into the mechanisms.[27,29,31–34] Tan *et al.* revealed that the smaller ΔE in Mn-doped PbTe is due to the anti-bonding of Te-*p* and Mn-*d* orbitals which push the second Σ pocket upwards.[34] The mechanism for other dopants with no *d* states near the Fermi level, such as Mg, Cd, is still unknown. The type-II band alteration—the resonant level—can also increase the band edge DOS as shown in Figure 2d. The aim is to have a dopant that forms the defect state in the vicinity of the Fermi level.[35,36] Such dopants usually have their electronic configuration very close to that of the host, such as when doping by elements from the neighbouring columns of the periodic table. Examples are IIIA elements doping in the rock-salt IV–VI structure and functioning as *p*-type dopants,[36–39] and IVA elements in V_2VI_3 compounds.[40] Pb doping on the Bi-site in BiCuSeO,[41] Sb-doping on the Te-site in $CuGaTe_2$,[42] and even antisite defects in ZrNiSn[43] are all known to form resonant levels at the respective band edges, illustrating a variety of resonant levels one can achieve in TE materials.

Beside the above-discussed mechanisms, the lower dimensional DOS caused by the Rashba spin-splitting effect and thus the larger *S* in comparison with predictions based on the SPB model were reported recently,[44] indicating another interesting approach to modify the DOS distribution around the Fermi level. Having more compounds with converged bands enhances chances of discovering TE materials with higher power factors. As the experimental determinations of the DOS are subject to uncertainties and technical challenges,[14,45] accurate *ab initio* band structure calculations are a convenient approach to inquire about the prospect of band convergence in a particular TE material and, no doubt, such calculations could have an even more prominent role in future studies.

Manipulation of carrier scattering

Carrier scattering is an indispensable part of electrical transport. The carrier relaxation time is determined by several scattering mechanisms, including electron–phonon scattering (both acoustic and optic phonon modes may participate), impurity scattering (both neutral and ionised), energy barrier scattering, piezoelectric scattering and electron–electron scattering. As shown in equation (5) and Figure 1b, each scattering mechanism can be expressed in terms of an energy-independent prefactor τ_0 and an exponential term ε^r where *r* is the scattering parameter. Different scattering mechanisms are expressed through different forms of the scattering parameter. For instance, for charge carriers scattered by acoustic phonons the scattering parameter $r = -1/2$, whereas for their scattering by ionised impurities $r = 3/2$. The carrier scattering can be altered by either the intensity of scattering events (prefactor τ_0) or by changing its energy dependence (scattering parameter *r*), both manipulations referred to as scattering engineering.

Given the expected operational range of TE materials used for power generation, acoustic phonon scattering is usually the dominant mechanism. Its scattering rate under the SPB model is,

$$\frac{1}{\tau} = \frac{1}{\tau_0}\varepsilon_F^{\frac{1}{2}} = \frac{\sqrt{2}E_{def}^2(m^*)^{\frac{3}{2}}k_BT}{\pi\hbar^4 v_s^2\rho}\varepsilon_F^{\frac{1}{2}} = \frac{\pi E_{def}^2 k_B T}{\hbar v_s^2 \rho}N(\varepsilon_F), \quad (7)$$

where E_{def}, $\hbar$, v_s, and ρ are the effective deformation potential for the electronic states, the reduced Planck constant, the sound velocity and the density of the material, respectively. In order to increase τ_0, the focus is usually on the reduction of the band effective mass m^* or DOS at the Fermi levels, the parameters that are more easily manipulated than the deformation potential or the sound velocity. Yang *et al.*[46] studied possible solutions for the relatively low mobility in Fe-based *p*-type skutterudites, and theoretically proposed the usage of 4*d* or 5*d* elements with which to form *p*-type skutterudites. The 4*d* or 5*d* electrons are spatially more delocalised, resulting in a lighter valance band and higher

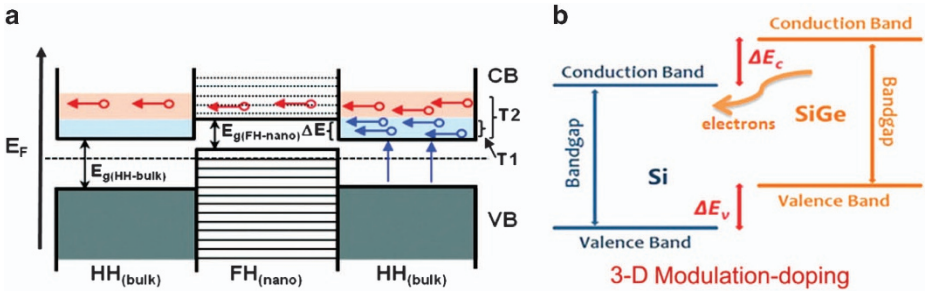

Figure 3. (**a**) Energy filtering effect in the half-Heusler/full-Heusler composites consisting of the half-Heusler matrix with the full-Heusler nanophase.[60] (**b**) Modulation doping in a two-phase nanocomposite consisting of the $Si_{95}Ge_5$ matrix and a large fraction of phosphorus-doped high Ge content $Si_{70}Ge_{30}P_3$ nanophase.[62]

mobilities. Fu *et al.* found experimentally that the *p*-type half-Heusler compound NbFeSb has a larger power factor enhancement than its isoelectronic cousin VFeSb due to the reduced effective mass and thus higher mobility.[47] The reduced effective mass in NbFeSb can be rationalised owing to stronger Nb 4*d*–Fe 3*d* interaction than 3*d*–3*d* one in VFeSb, similar to a situation in light valence band skutterudites. Other experiments emphasising the importance of low DOS in order to achieve high-carrier mobility are I-doped PbTe[48] and K-doped BiCuSeO.[49] Improved power factors can be obtained by a successful tradeoff between the mobility enhancement and a reduction in the Seebeck coefficient.

The enhancement of the Seebeck coefficient by enhancing the scattering exponent *r* is another aspect of the scattering engineering. The SPB expression for the Seebeck coefficient in the degenerate doping limit is,

$$S = \frac{k_B^2 \pi^2 T}{3e\varepsilon_F} \cdot \left(\frac{3}{2} + r\right). \quad (8)$$

This effect is usually achieved by introducing additional scattering centers, e.g., ionised impurities that force the scattering parameter to change from −1/2 to +3/2. Several experimental works have supported this idea, among them the research with doped skutterudites,[50–53] Ni cross-substituted type-I clathrates,[54] and Bi_2Te_3 with native defects.[55] This change of *r* brings about additional scattering, which inevitably reduces the mobility. Finding a proper ratio between the acoustic phonon scattering and the impurity scattering is essential to maximise the benefits. For instance, Dyck *et al.* adopted a two-scattering-mechanism model, considering both the acoustic phonon and ionised impurity scattering, to deduce the optimal power factors of Ni-doped Ba-filled $CoSb_3$.[50] Similar procedure has been adopted in Cr-doped Ce-filled $CoSb_3$.[53] Both the enhanced ionised impurity scatterings and the charge compensation effects (increasing the filling fraction limits of Ce) of the dopant Cr are beneficial to the averaged ZT values.

Energy barrier scattering also involves the use of strongly energy-dependent scattering to enhance the Seebeck coefficient. It can be done by introducing interfaces in a composite structure that have energy barriers, which block carriers at low energy but not those at high energy.[56] Energy-barrier scattering is conceptually similar to the scattering by ionised impurities; both processes scatter low-energy carriers more effectively than the high energy ones, but the implementation is different. The beneficial effect of energy barriers can be found in the systems having a semiconducting host matrix and metallic composites or nano-inclusions, such as the pristine PbTe matrix containing Ag-doped PbTe nanoparticles,[57] semimetallic ErAs particles in InGaAs/InGaAlAs superlattices,[58,59] and half-Heusler compounds with full-Heusler metallic inclusions (Figure 3a).[60,61] Another possible beneficial scheme relating to the interface between matrix and nanostructure is the modulation doping and *δ*-doping techniques. In principle, it is different from the barrier scattering mentioned above since the dopants are only incorporated into certain areas, e.g., spatially separated nanograins, leading to reduced electron scattering and thus higher mobility. Improved power factors and figure of merit ZT are experimentally achieved in the $Si_{95}Ge_5$ matrix and the phosphorus-doped $Si_{70}Ge_{30}P_3$ nanoparticle phase, where the electrons can spill over from the doped nanoparticle phase into the essentially undoped matrix phase, as shown in Figure 3b.[62]

Another strategy on how to apply scattering engineering might be found in topological insulators having a large difference in the relaxation times corresponding to bulk and surface states. As the surface states are topologically protected, at the energy interface between surface and bulk states there is an abrupt change in the relaxation time. Xu *et al.*[63] proposed a dual-scattering time model for TE transport tuning in topological insulators. Their model calculations show that the ratio between the surface and bulk states has an important role in the figure of merit ZT, and ZT values of over 8 might be achieved when the ratio is $>10^3$ in two-dimentional topological insulators. Shi *et al.*[64] also connected the topological insulator property to TE performance based on calculations for Bi_2Te_3 and Bi_2Te_2Se, more from the band complexity point of view. Up to now, it is still an open question whether the topologically insulating behaviour is beneficial to thermoelectrics, as well as the origin of the benefits (from scattering or band variations) if there is any.

In general, scattering engineering offers exciting possibilities for enhancing TE performance. The power factor can be enhanced by a more rapid energy dependence of the relaxation time, by introducing defects or interfaces with energy barriers that filter out low energy carriers, and by using innovative modulation doping schemes that promote high carrier mobilities. Although the intent is clear, the realisation of the above scattering engineering approaches is quite challenging. More research is needed to understand the rationale regarding to the microscopic mechanisms leading to the desired changes in the scattering parameter.

Carrier conductive network

In 1995, Slack proposed an architecture for high-ZT ternary compounds in which the vast majority of atoms formed a conductive framework for charge carriers, while the chief role of the remaining atoms was to scatter phonons.[9] This PGEC paradigm was very influential in the discovery of several families of TE materials. It also presented a novel architecture, which was distinctly different from the traditional TE compounds such as PbTe, Bi_2Te_3 and so on, in which all the component elements were responsible for the electrical transport. It was not recognised initially that the PGEC paradigm also contained a concept of conductive networks. Strictly speaking, electronic structures of crystalline solids possess contributions from the electronic orbitals of all atoms. However, since the effective energy windows for

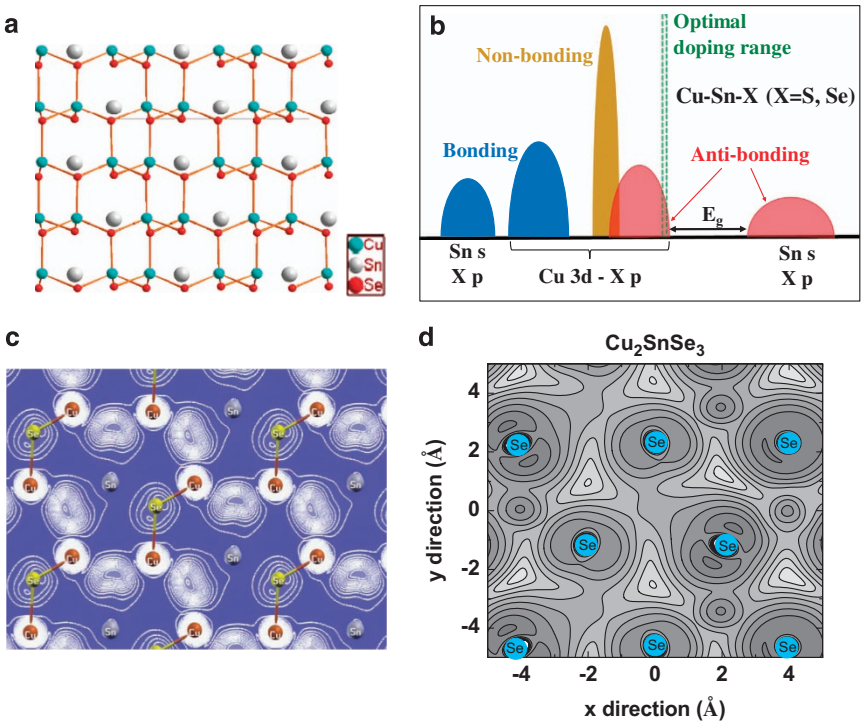

Figure 4. (**a**) The crystal structure of Cu_2SnSe_3. (**b**) The scheme plot of DOS in Cu_2SnX_3 (X = S, Se), with the bonding characters and the *p*-type optimal doping range labeled. (**c**) and (**d**) are the contour plots of the partial charge density within the *p*-type optimal doping range of Cu_2SnSe_3 (−0.2 to −0.3eV) on the Cu–Se–Sn plane,[72] and the close-packed Se–Se–Se plane, respectively.[71]

electrical transport are narrow (Figure 1), the concept of conductive networks is approximately valid when those atoms forming the network dominate the electronic states of interest. On the basis of the experience gained with various TE compounds in the recent years, several well-accepted qualitative features have emerged that speak strongly for the usefulness and validity of the concept of conductive networks based on both theory and experiment, as will be shown in the following.

N-type filled $CoSb_3$-based skutterudites are regarded as prototype compounds that embody the PGEC concept. The conduction band minimum (CBM) of pure $CoSb_3$ is composed of *d*–*p* hybridised orbitals of both framework elements.[65] The guest fillers, usually very metallic cations, form ionic bonds with the surrounding Sb atoms, and do not affect the CBM of $CoSb_3$ except for shifting the Fermi level position.[66,67] Experimentally, the rigidity of the CBM is reflected by the influence of fillers on the transport parameters. As shown in ref. 68, the experimental Seebeck coefficients of skutterudites with various fillers and filling fractions follow the same Pisarenko relation; and the electron mobilities have the same −3/2 temperature dependence. Thus there exists a universal optimal doping level for *n*-type filled skutterudites (~0.5 electrons per Co_4Sb_{12} cell at 850 K), simplifying the optimisation in experiments especially for multiple-filled systems.[67,69] The conductive networks in *p*-type Fe-based skutterudites were also studied by Yang *et al.*,[70] with the conductive network mainly composed of *d* orbitals from Fe.

The concept of conductive networks is not limited to the caged structures. Xi *et al.* studied electronic structures and chemical bonding in diamond-like compounds $Cu_2SnS(Se)_3$ (Figure 4a).[71] On the basis of the analysis of the bonding character, the bands constituting the valence-band maximum (VBM) are mainly composed of the anti-bonding between Cu *d* and Se *p* orbitals, and contain no obvious contribution from Sn atoms (Figure 4b). The energy range corresponding to the maximum *p*-type power factor is close to the VBM (around 0.1 hole per formula unit in the case of Cu_2SnSe_3), as labelled in Figure 4b. In this optimal doping range, there exist a 3D [-Cu-Se(S)-Cu-] conductive network with Cu-Se(S) anti-bonding (Figure 4c),[72] as well as a closely packed chalcogenide framework (Figure 4d),[71] and both of them contribute to the hole transport. In either of the network, Sn is isolated. Doping on the reservoir element Sn in these compounds for maximising the electrical properties is desirable,[72] owing to the undisturbed conductive networks. The Cu 3*d*-chalcogen *p* hybridised bond forming the VBM is universal in Cu-based diamond-like compounds and similar conductive networks have been revealed by calculations for other diamond-like compounds.[73,74]

The above studies reveal some general qualitative features of conductive networks in TE materials. At the Fermi level, atoms on the conductive network form a clear bonding channel in real space, with out-of-network atoms being nearly isolated. In the energy space, the electronic states at the Fermi level are derived from the corresponding network atoms, with little contribution from other species. This makes it possible for the out-of-network atoms to serve as a carrier reservoir. Tuning and modification of the carrier reservoir will change neither the band structure nor the scattering mechanism. The optimal doping levels can be easily obtained based on the bulk bands, an approach which is very useful for experimental optimisation. From the chemical bond perspective, compounds with conductive networks usually possess the so-called chemical bond hierarchical structure. The out-of-network atoms are typically loosely bonded with the rest of the structure with large atomic displacement parameters (ADPs), and giving rise to low-frequency resonant phonon modes. The topic will be discussed in 'Resonant phonon scattering and low-frequency rattling modes' and 'Diverse lattice dynamics and part-crystalline part-liquid state in complex thermoelectrics'. Owing to these beneficial features, it is advisable to carry out the identification of conductive networks in more complex compounds. Besides the filled skutterudites and diamond-like compounds, many Zintl compounds are another type of structure

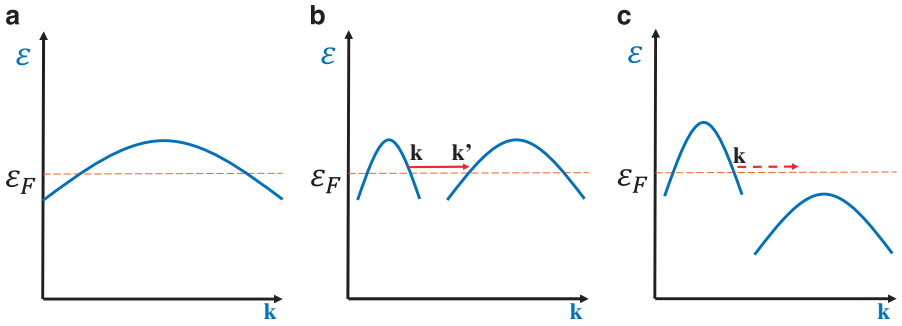

Figure 5. The comparison of three band schemes, (**a**) a single heavy band; (**b**) energy converged multiple bands; (**c**) energy separated multiple bands.

with a well-defined conductive network, in this case composed of the polyanion sublattice.[75–78]

Theoretical description of electrical transport and challenges

So far, we have reviewed three topics concerning the electrical transport: band engineering; scattering engineering; and conductive networks in complex compounds. The first two are primarily aimed at the power-factor enhancement by the manipulations on either the band structure or the carrier scattering. Conductive networks are an idealised architecture for complex TE materials, where only a part of the structure contributes to the electrical transport. Applications of these three topics in a variety of TE materials were discussed in 'Band engineering for enhanced power factors', 'Manipulation of carrier scattering' and 'Carrier conductive network'; here we will focus on the theoretical understanding and the challenges ahead.

Electrical transport could be described within the framework of the Boltzmann transport theory. One basically inquires how the distribution function evolves under external fields. Relevant formula are presented at the beginning of 'Electrical Transport in Thermoelectrics'. Comparing the definition of σ (equations (2) and (4)) with the macroscopic form of $\sigma = ne\mu$, the integral of the DOS is equivalent to n, and therefore the carrier mobility is directly related to the integral of the relaxation time $\tau_{i,\mathbf{k}}$ and the group velocity,

$$\mathbf{v}_{i,\mathbf{k}} = \frac{1}{\hbar}\nabla_{\mathbf{k}}\varepsilon_{i,\mathbf{k}}. \tag{9}$$

Dispersive bands and low scattering rates are favourable for high μ. The Seebeck coefficient S, due to the cancelling effect at both the denominator and numerator, is less sensitive to $\mathbf{v}_{i,\mathbf{k}}$ or $\tau_{i,\mathbf{k}}$. This is the foundation of the constant relaxation time approximation (CRTA) and thus τ-free S in many of the methodologies for electrical transport calculations nowadays. The term $(\varepsilon-\varepsilon_F)$ in equation (3), however, implies that S is sensitive to the changing rates of TDF $\overline{\sigma}(\varepsilon)$ on both sides of the Fermi level, as already mentioned in the context of band engineering and scattering engineering.

The influence of band engineering on power factors can be fully understood after taking both S and μ into account. For example, one single heavy band (Figure 5a) or multiple energy converged bands (Figure 5b) with equivalent DOS effective masses could have the similar Seebeck coefficients but rather different mobilities due to the different $\mathbf{v}_{\mathbf{k}}$. For systems that already possess multiple bands, achieving the band convergence is beneficial from the DOS point of view, in which the system still keeps the same $\mathbf{v}_{\mathbf{k}}$, as shown in Figure 5b,c. However, one thing that might be detrimental to the mobility is the carrier intervalley scattering (Figure 5b). The energy degenerate bands do increase the scattering channels for carriers, which could increase rates for all possible scattering mechanisms. Experimentally, the mobility values for large band degeneracy systems are lower than for systems with lower band degeneracy at comparable carrier concentrations.[14,28]

A comprehensive band engineering approach to evaluate effects influencing the power factor should consider intervalley scattering processes caused by the high-band degeneracy. Direct calculations of the intrinsic electron–phonon scattering based on full electron and phonon dispersions have been realised only in the recent years.[79,80] The inverse relaxation time for an electron state at $\mathbf{k}$ being scattered by a phonon $\mathbf{q}$ can be written as,

$$\frac{1}{\tau_{\mathbf{k}}} = \frac{2\pi}{\hbar}\sum_{\mathbf{k}'}\left|\langle\mathbf{k}'|\partial_{\mathbf{q}}V|\mathbf{k}\rangle\right|^2[(f_{\mathbf{k}'}+n_{\mathbf{q}})\delta(\varepsilon_{\mathbf{k}}-\varepsilon_{\mathbf{k}'}+\hbar\omega_{\mathbf{q}})\delta_{\mathbf{k}+\mathbf{q},\mathbf{k}'+\mathbf{G}} + (1-f_{\mathbf{k}'}+n_{\mathbf{q}})\delta(\varepsilon_{\mathbf{k}}-\varepsilon_{\mathbf{k}'}-\hbar\omega_{\mathbf{q}})\delta_{\mathbf{k}-\mathbf{q},\mathbf{k}'+\mathbf{G}}]\left(1-\frac{\mathbf{v}_{\mathbf{k}'}\cdot\mathbf{v}_{\mathbf{k}}}{|\mathbf{v}_{\mathbf{k}'}||\mathbf{v}_{\mathbf{k}}|}\right). \tag{10}$$

Here $n_{\mathbf{q}}$ and $\omega_{\mathbf{q}}$ are the phonon number and the phonon frequency, respectively. $\left|\langle\mathbf{k}'|\partial_{\mathbf{q}}V|\mathbf{k}\rangle\right|$ is the scattering matrix, which is the key element in the calculation. Implementation of such method could be helpful for better quantification of the effects from band engineering. It is, however, a very demanding undertaking and rarely carried out. For other scattering mechanisms, to our best knowledge, there is no direct calculation reported so far.

The limited knowledge concerning various scattering processes also impacts attempts to do scattering engineering, which is currently beyond the theoretical capability. From experiments, the relative strength of multiple scattering mechanisms is commonly extracted by fitting the Pisarenko plot (S versus n). A more direct way to measure the scattering parameter r is to use the so-called 'four coefficients' method, i.e., from the measurements of four transport coefficients to determine another four microscopic parameters, including the scattering parameter r.[38,81,82] The 'four coefficients' method should be used with more systems to shed light on the underlying physical processes that cause variations in the scattering processes. Other strategies for scattering engineering, such as the carrier barrier scattering and nanoinclusions, currently lack any microscopic understanding.

The concept of conductive networks is an approximation in which, within the energy window of interest, only parts of the compound contribute to the electrical transport. Several qualitative descriptions have already been provided in 'Carrier conductive network'. The currently used theoretical approaches which describe conductive networks are the dominant contributions for in-network atoms from electronic structures. These, however, may not necessarily be the same as contributions to the electrical transport. A more accurate and definitive theoretical approach that can directly relate the electrical transport properties to the atomic species is needed. The task is interesting but challenging, especially when considering the fact that the loosely bonded out-of-network atoms may lead to structural fluctuations.

THERMAL TRANSPORT IN THERMOELECTRICS

As mentioned, the thermal conductivity κ has three components, the electronic part κ_e, the lattice part κ_L, and the bipolar part κ_{bi}. The κ_e links with σ via the Windeman–Franz law $\kappa_e = L\sigma T$. The Lorenz number L in semiconductors varies between 1.5 and $2.44\times10^{-8}\,W\Omega\,K^{-2}$, spanning the range from non-degenerate semiconductors to strongly degenerate systems. The κ_{bi}, which arises as a consequence of electron–hole pair creation at the hot side of a sample and its recombination at the cold side, depends on the ratio of mobilities for majority and minority carriers in the non-degenerate case[83,84] and on the minority conduction only in degenerate case.[85] In order to suppress the bipolar contribution to the κ in degenerate semiconductors, it is desirable to reduce the minority carrier transport. This can be achieved by the band alteration, such as increasing the band gap, reducing the minority effective mass and so on, or by the preferential scattering of the minority carriers, as proposed by Wang *et al.*[85] In this section, however, we shall focus on the discussion of the lattice thermal conductivity κ_L, the dominant contribution to the heat transport in thermoelectrics for most of the cases.

In a conventional crystalline solid, the lattice thermal conductivity is determined by the specific heat capacity c, the sound velocity v_s, and the mean free path (MFP) l or phonon relaxation time τ_q according to $\kappa_L = \frac{1}{3}cv_sl = \frac{1}{3}cv_s^2\tau_q$. The respective parameters entering the above equation and, specifically, the phonon relaxation time τ_q are frequency dependent.[86,87] Figure 6 presents the phonon scattering times for various mechanisms as a function of phonon frequency. Among these, PPIs are an intrinsic mechanism. Of the extrinsic mechanisms, the grain boundary scattering is nearly independent of frequency and influence mainly the transport of long-wavelength phonons. Point defects are particularly effective in scattering high frequency phonons on account of their ω^4 frequency dependence (Rayleigh scattering). Nano-inclusions, behave approximately as point defects for low-frequency (long wavelength) phonons, and as grain boundaries for short wavelength phonons. Some of these traditional scattering mechanisms will be discussed in 'From the conventional phonon–phonon interactions to nanostructures'.

Large atomic displacements of guest fillers in compounds with open crystal structures make them interesting and unique. The physical origin of substantial reduction of the κ_L achieved in these materials with void fillers, i.e., the rattling induced resonant scattering at low frequencies (Figure 6) or merely alterations of the phonon spectrum, has been debated for a long time. These topics will be presented in 'Resonant phonon scattering and low-frequency rattling modes'. We will also review those compounds with some atoms having very large atomic displacements and even liquid-like behaviours in 'Diverse lattice dynamics and part-crystalline part-liquid state in complex thermoelectrics'. The dynamic behaviours of these atoms and the associated phonon

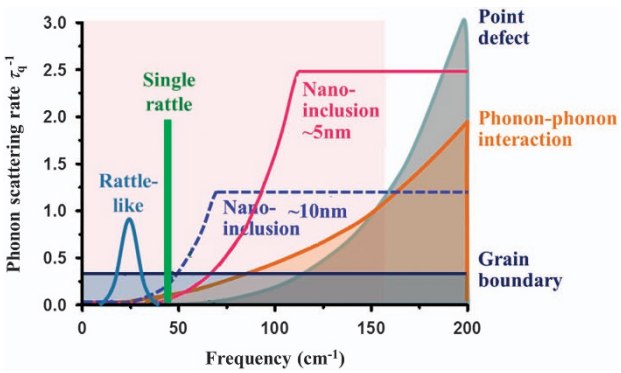

Figure 6. Schematic plot demonstrating the frequency dependence of phonon scattering rates for various mechanisms.

scattering mechanisms owing to the large atomic displacements fall beyond the conventional treatment relying on small parameter perturbative theory. How to properly describe the heat transport in these compounds is still an open question.

From the conventional phonon–phonon interactions to nanostructures

The traditional ways to achieve low κ_L in TE materials is to use heavy constituent elements or complex structures with low phonon velocities or reduced fractions of heat-carrying phonons.[1,88,89] Solid solutions are another time honored approach to enhance point defect scattering.[90–95] PPIs, as the intrinsic mechanism and basically the dominant one at high temperatures, have offered limited opportunities for regulation. Recently, thanks to advanced computational capabilities, the understanding on PPIs and their influences on lattice thermal conductivity has been greatly improved. Among the extrinsic scattering mechanisms, nanostructures have been widely used in TE materials due to the significant effect on scattering long-wavelength phonons which are difficult to scatter otherwise. In this subsection, the focus will be on PPIs and the role of nanostructures.

PPI is an intrinsic process taking place in all crystalline solids and is robust to doping, alloying, grain size and so on. Large lattice anharmonicity, characterised by the effective Grüneisen parameter γ, and low group velocity are common explanations for low κ_L under strong PPIs.[86,96] In addition, as revealed by the recent *ab initio* third-order interatomic force constant (IFC) calculations, a large scattering channel, analogue to the electronic DOS in the carrier scatterings (equation (7)), can serve as another approach to obtain a strong PPI.[97] Binary chalcogenide compounds have served as a target of many theoretical studies aimed at the understanding of their low κ_Ls.[24,98–102] An *et al.*[98] and Zhang *et al.*[100] revealed that the very soft transverse optic phonon at Γ point in PbTe, responsible for the low κ_L of the compound, is caused by the near ferroelectricity and the partially covalent character of Pb–Te bond. The covalent character was further highlighted by Lee *et al.*[102] who found strong resonant bonding in IV–VI rock-salt chalcogenides. These resonant bonds result in large anharmonicities, optic phonon softening and large scattering channels, all favourable for low lattice thermal conductivity.[101–103] The deformed rock-salt structure material SnSe was reported to show an exceptionally low in-plane κ_L, resulting in a record-high $ZT = 2.62$.[104] The *ab initio* calculations reveal that the strong PPI of SnSe originates from the large phonon scattering channel and the very anharmonic resonant bonds.[103,105]

Recent molecular dynamics calculations of PPI even account for the evolution of κ_L with temperature. The stiffening of the transverse optic phonon at Γ point in PbTe with increasing temperature is revealed by both inelastic neutron scattering and AIMD calculations.[106,107] The transverse optic phonon and longitudinal acoustic phonon are decoupled at 600 K, which reduces the scattering channel and causes the kink in high temperature κ_L. The opposite case is presented by Bi_2Te_3 where more optic phonons are involved in scattering when the temperature increases and thus the decrease of κ_L is faster at room temperature.[108]

The above studies emphasise the several factors causing strong PPI and low κ_L. Those zone center acoustic phonons, however, whose wavelengths are usually longer than the scales of unitcells, are hard to be scattered by PPI due to their low frequencies and small wave vectors. Nanostructures, including nanometer scale grains, nanoinclusions and nanocomposites, thus need to be considered in order to achieve interface scattering to long-wavelength phonons. A representative example is the concept of 'all-scale' phonon scattering by the integrated length scale of microstructures.[109] By using different amounts of SrTe, Biswas *et al.* introduced atomic scale solid solutions, nanoscale

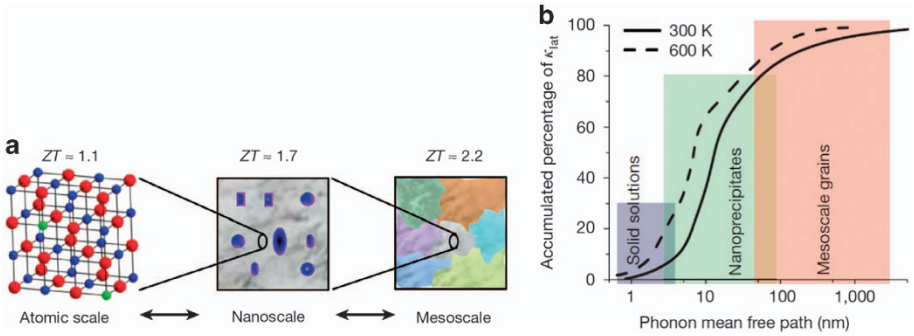

Figure 7. (**a**) All scale phonon scattering by the microstructure design in the PbTe-SrTe composite system.[109] (**b**) Accumulated κ_L of PbTe as a function of phonon mean free path.[109]

precipitates and mesoscale grain boundaries into PbTe (Figure 7a), and increased the ZT values correspondingly. Over the years, the benefits of nanostructuring on κ_L reduction have been well-accepted. The vital issue with the use of nanostructures is the lack of accurate size and shape control of grains, as well as a quantitative and insightful theory. This makes the nanostructures only a qualitative explanation for the κ_L reduction.

The foundation element of the all-scale phonon scattering paradigm is the accumulated fraction of the thermal conductivity with respect to the phonon mean-free path (Figure 7b). On the other hand, charge carrier mobilities will also be interfered with by the much enhanced density of interfaces. Thus a proper control of the nanostructure scale is necessary to preferentially scatter phonons. It is essential then to know both the critical lengths (i.e., the wavelength or the mean free path) of electrons and phonons. Yang *et al.* calculated the room temperature values of the electron de Broglie wavelength λ,[110] and the values of λ for degenerate compounds fall within a narrow range ($\leqslant$5 nm). The phonon mean-free paths, if we define the mean values corresponding to 50 % κ_L reduction,[111] vary by 2–3 orders of magnitude according to *ab initio* IFC calculations.[94,102,105–108] Usually, low κ_L materials have low MFPs, sometimes even lower than the effective length of charge carriers. This makes the nanostructuring approach less effective for low κ_L materials, as verified by the theoretical work with nanoparticles embedded in $(Bi, Sb)_2Te_3$.[112] Only compounds with long MFPs of phonons, such as Si or SiGe alloys, half-Heusler alloys, and skutterudites, can sufficiently take the benefits from the nanostructures. Furthermore, owing to the decreasing of MFP of phonons as the temperature increases (Figure 7b),[109,111] the effect on the κ_L from the interface scattering will diminish at higher temperatures.

Another quantitative effort is the modelling of κ_L variations due to modulations of the nanostructure. Simulations on different length scales, using the methods from *ab initio* calculations to molecular dynamics with empirical potentials, have revealed a strong influence on κ_L by nanocomposites possessing complex geometry, usually fabricated within the Si–Ge system. The κ_L is typically determined by the surface area and the volumetric fraction of the composite, as shown by the study with different types of Si nanowires embedded in the Ge host.[113,114] Size effects in the phonon transport of Ge containing Si nanoparticles were emphasised by the Monte Carlo simulation.[115] Several studies documented the optimal sizes and distributions in the nanocomposites.[116–119] Mingo *et al.* studied 17 different silicide nanoparticles in the SiGe host,[116] and revealed the existence of the optimal nanoparticle size that minimises the nanocomposite's κ_L. Similarly, the optimal Si/Ge superlattice period of around 3.3 nm minimised the value of the κ_L.[117] Besides the focus on κ_L, calculations were also made to estimate ZT values for some composite systems such as SiGe composites, nanotubes and quantum dot superlattices.[120–122]

A great progress has been achieved in reducing the κ_L by scattering phonons over a wide range of frequencies. Advances in computational methodologies have been instrumental in promoting the understanding of the lattice dynamics in TE materials as exemplified by prolific studies of PbTe. The calculations also indicated the proper nanostructure size effective to preferentially scatter long-wavelength phonons. Modelling work has helped to rationalise the role of complex nanocomposites on κ_L. On the basis of the above studies, the understanding of the phonon transport in conventional materials has been clarified to a large extent even though the full quantitative prediction is still a challenge.

Resonant phonon scattering and low-frequency rattling modes

In 'From the conventional phonon–phonon interactions to nanostructures', we have seen the great influence on the κ_L exerted by extrinsic scattering mechanisms such as nanostructures, as well as the improved understanding of intrinsically strong PPIs. Then an interesting question arises concerning whether it is possible to find structures where some other 'intrinsic' process for low κ_L might exist, and do so with a high degree of adjustability like nanostructures? Moreover, if such desired structures existed, would it still be possible to use small-perturbative phonon approximation to describe the thermal transport properties in the structures?

As a kind of compounds transiting from the conventional to the unconventional materials are compounds with an open crystal structure, such as skutterudites and clathrates. These compounds possess large structural voids that can be filled with loosely bonded foreign species, which have a strong influence on the κ_L. Filled skutterudites were first synthesised by Jeitschko and Braun[123] and they became a target of intense scrutiny as TE materials in the late 1990s.[124–126] Compared with the conventional compounds with the chemical-bond homogeneity, the fillers possess much larger ADPs compared with the atoms forming the framework, leading to chemical-bond hierarchy and much reduced κ_L. Nolas *et al.*[127] found that the point defect scattering is not sufficient to explain the very low κ_L in partially filled skutterudites. The resonant scattering mechanism, in which acoustic phonons are scattered by the resonant vibrations of the fillers, was thus proposed. A typical form of the scattering rate under this scattering mechanism is,[128]

$$\frac{1}{\tau_{Res}} = \frac{C\omega^2}{\left(\omega^2 - \omega_0^2\right)^2}. \quad (11)$$

Here C is a constant proportional to the concentration of the resonant centers, which oscillate with the frequency ω_0. Various filler species in Co_4Sb_{12} with characteristic resonant frequencies were explored subsequently.[129,130] The reduction of κ_L by rattling fillers in the filled skutterudites could be achieved over a wide temperature range, as shown in Figure 8a. This is a very effective

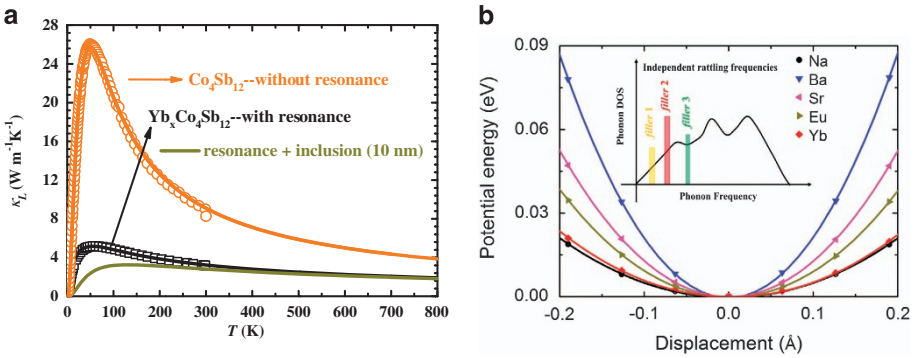

Figure 8. (**a**) The evolution of κ_L from pure Co_4Sb_{12} (without resonance), to $Yb_xCo_4Sb_{12}$ (with resonance) and to the calculated $Yb_xCo_4Sb_{12}$ containing 10 nm nano-inclusions. (**b**) Schematic plot for the resonant scattering and the potential well for different fillers in $CoSb_3$. Data are from ref. 131.

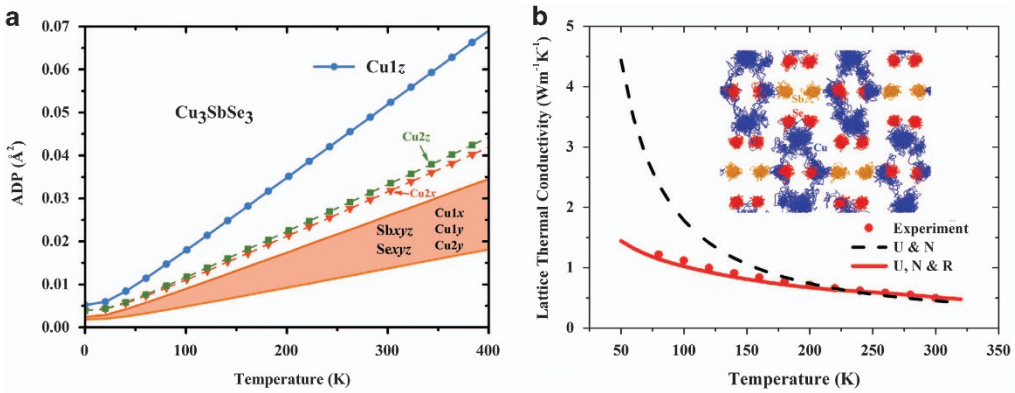

Figure 9. (**a**) Atomic displacement parameters of all constituent elements of Cu_3SbSe_3. (**b**) The lattice thermal conductivity with and without the rattle-like scattering term (R) in the same compound. Data are from ref. 147.

way of realising the thermal conductivity reduction; even augmenting nanoinclusions into a $CoSb_3$ matrix can hardly give rise to a comparable reduction in a broad temperature range (Figure 8a). In 2007, Yang *et al.*[131] theoretically calculated the potential well for various fillers in Co_4Sb_{12} (Figure 8b), and determined their resonant frequencies using a harmonic approximation. On the basis of the results, using multiple fillers with significantly different resonant frequencies was proposed as a method to obtain a further reduction in κ_L. Experimentally, the so-designed multiple-filled skutterudites do possess reduced κ_L and enhanced *ZT* values, as shown in refs. 68,69,132,133. Resonant frequencies of fillers in *p*-type skutterudites were also calculated by Liu *et al.*[134] and used to design high-performance *p*-type skutterudites.

Despite the great success in guiding the experiments, the resonant scattering mechanism itself has often been questioned. On the basis of the neutron spectroscopy experiments and *ab initio* lattice dynamic calculations for the fully filled $La(Ce)Fe_4Sb_{12}$, Koza *et al.*[135] argued that the guest fillers should couple with the host atoms in a coherent way, and show an ordinary phonon behaviour of filler species rather than the independent rattling motion. The κ_L reductions should be attributed to the zero group velocities of the low-frequency optic phonon branches. Christensen *et al.* demonstrated the acoustic-optic interaction and avoided-crossing behaviour of phonons in another cage structure, $Ba_8Ga_{16}Ge_{30}$ clathrate, using neutron triple-axis spectroscopy.[136] The reduction of phonon relaxation time caused by the additional optic phonons is inadequate to explain massive suppressions in κ_L, hence, the influence of the reduced group velocity was invoked. The importance of reduced group velocity of phonons was further discussed in refs. 88,137. Subsequent experimental and *ab initio* work also confirmed the presence of acoustic–optic interactions in skutterudites.[138,139]

The above-mentioned controversy focuses mainly on the exact role of fillers in reducing the κ_L. With fillers introducing the nearly zero-velocity optic phonon modes at certain frequencies is phenomenologically equivalent to the resonant scattering mechanism proposed earlier. It is worth noting that suppressions of κ_L by the fillers cannot be fully accounted for by the introductions of additional optic phonons, based on the third-order IFC calculations.[111,140,141] The κ_L for the unfilled $CoSb_3$ can be perfectly reproduced by these calculations;[111] for fully filled skutterudites, however, the theoretically estimated κ_Ls turn out to be either too high such as that for $BaFe_4Sb_{12}$, or too low such as that for $YbFe_4Sb_{12}$.[141] In addition, the largest κ_L reduction due to the fillers are observed to appear at about 30 K, and this also cannot be rationalised solely by the variations of phonons, either. Heat transport in open structure materials with guest fillers seems to be complicated and still requires more research efforts.

The rattling motion of guest fillers in clathrates is usually viewed as similar to the case in filled skutterudites. Interestingly, relatively small fillers, such as Sr and Eu in Ge-based clathrates or Ba in Sn-based clathrates, have the off-center rattling character, with fillers tunneling among the off-center-sites.[142–144] The unique behaviour results in flat and broad range of optic phonons in the dispersion relations and glass-like κ_L at low temperatures.[144] Another good example of rattling modes was found in sodium cobaltate by Voneshen *et al.*[145] The Einstein-like rattling modes were caused by the sodium vacancies. The rattling modes suppress κ_L by a factor of six. All of these compounds belong to a more common chemical-bond hierarchy architecture. The identification of this hierarchy architecture in more compounds are desirable, both for practical and physical interests.

Diverse lattice dynamics and part-crystalline part-liquid state in complex thermoelectrics

The resonant term (equation (11)) describing the rattling behaviour indicates the phonon transport in caged open structure compounds has already gone beyond the conventional crystalline solids. Hierarchically bonded architectures are not limited to the caged compounds; several compounds with other crystalline symmetries are reported to have quite distinct strong–weak bonding hierarchy.

Qiu *et al.* investigated the lattice dynamics and thermal transport behaviour of Cu–Sb–Se compounds, Cu_3SbSe_4, $CuSbSe_2$ and Cu_3SbSe_3, containing identical constituent species in different crystal structures.[146] Their work pointed out differences between crystalline and part-crystalline materials. For Cu_3SbSe_4 and $CuSbSe_2$, all atoms are confined to vibrate around their equilibrium positions. In Cu_3SbSe_3, however, Cu atoms oscillate with very large ADPs along certain specific directions (Figure 9a). If adopting the Lindemann melting criterion, then specified by the dimensionless Lindemann parameter δ ($\delta = \sqrt{\mathrm{ADP}}/R_{\mathrm{NN}}$, R_{NN} is the nearest-neighbour distance) exceeding 0.07, the Cu-sublattice could be considered as melted above 400 K (Figure 9a). The entire compound is thus in a special part-crystalline part-liquid hybrid state at elevated temperature, representing the atomic-level heterogeneity.

The measured temperature dependence of the κ_L of Cu_3SbSe_3 (Figure 9b) strongly deviates from the classical T^{-1} behaviour.[147] An effective rattle-like thermal damping term (Figure 6) is phenomenologically added to the denominator of equation (11), which can describe the reduction and the unique temperature dependence of the κ_L perfectly (Figure 9b).[147] The local motion or vibration of the set of atoms leads to the collective broadband thermal damping term, different from the single rattling behaviour in filled skutterudites. Interestingly, Cu_3SbSe_3 is also reported to have an s^2 lone-electron pair in an earlier work, which seemingly offers another explanation of the low κ_L.[148,149] But the analysis of Qiu *et al.* revealed that the reduction in thermal conductivity is more from the structural factor instead of the lone-pair electrons.[147] In contrast, the κ_L of Cu_3SbSe_4 and $CuSbSe_2$ shows a T^{-1} relationship,[146] which can be successfully described by the traditional PPIs in perturbative theory.

An even larger Cu mobility can be found in the superionic Cu_2Se which has a liquid-like Cu sublattice.[150] The structure in Cu_2Se contains a static disordering as well as a fluctuating dynamic disordering due to its liquid-like structure feature. Using AIMD, Kim *et al.*[151] studied the temperature-dependent lattice dynamics of β-Cu_2Se. The Cu–Cu bond lengths are close to that in Cu metal, much shorter than those found in the ordered antifluorite structure. The calculated κ_L, based on the non-equilibrium AIMD, agrees well with the experiments. More results regarding Cu_2Se and related compounds will be reviewed in 'Synergistic optimisation for high ZTs'.

A part-crystalline part-liquid (amorphous) material, intrinsically exhibits the unusual lattice dynamics and attains an abnormally low κ_L due to its statically disordered substructure and the dynamically fluctuating sublattice. These new material types offer good TE properties and interesting physics, as well as challenges for theoretical and experimental descriptions of the transport issues. For instance, the perturbative theory for the κ_L treatment, and even the concept of a phonon, may become questionable for these materials. Proper theoretical methods accounting for the structural fluctuation should be developed. For experimentalists, the fluidity of the ions, such as Cu^+ in Cu_2Se, Cu_2S, presents an unpleasant realisation that the sample under study will likely degrade during measurements.[152] How to balance the extra-ordinary TE performance with the practicality is an open question.

Theoretical description of thermal transport in bulk thermoelectrics and challenges

The lattice thermal conductivity for conventional solids can be calculated based on the relaxation time approximation and the phonon gas model, considering contributions from each phonon **q**,

$$\kappa_L = \frac{1}{3}\sum_{\mathbf{q}} \hbar\omega_{\mathbf{q}} v_s^2 \tau_{\mathbf{q}} \frac{\partial N_{\mathbf{q}}^0}{\partial T}. \tag{12}$$

Here, $\omega_{\mathbf{q}}$, $\tau_{\mathbf{q}}$, and $N_{\mathbf{q}}^0$ are the phonon frequency, the relaxation time of phonons, and the equilibrium Bose–Einstein distribution function, respectively. An analytical model, taking into account the perturbed phonon population caused by normal process, was proposed initially by Callaway[153] and widely adopted in the study the κ_L for solids over the years.[147,154,155] The resistive scattering processes include grain boundary scattering (τ_B), point defect scattering (τ_{PD}), phonon–phonon Umklapp processes (τ_U), electron–phonon interaction ($\tau_{e\text{-}p}$), etc. The overall scattering rate is obtained by adding scattering rates of the individual scattering processes,

$$\frac{1}{\tau_{\mathbf{q}}} = \frac{1}{\tau_B} + \frac{1}{\tau_{\mathrm{PD}}} + \frac{1}{\tau_U} + \frac{1}{\tau_{e-p}} + \dots . \tag{13}$$

Variations in κ_L come mostly from the relaxation time.

Point defect scattering can affect mid-to-high frequency phonons (Figure 6). The coefficient of the scattering rate can be altered by mass and strain field fluctuations with the former being expressed as,[87]

$$\frac{1}{\tau_{\mathrm{PD}}} = \frac{\Omega}{4\pi v_g^3}\omega^4 \sum_i f_i \left(\frac{\overline{m} - m_i}{\overline{m}}\right)^2. \tag{14}$$

f_i is the fraction of atoms with mass m_i, and $\overline{m}$ is the average mass of all atoms. Point defect scattering is important for the κ_L variations in solid solution of TE material systems as already mentioned,[90–95] as well as in the isotope effect.[97,156] It is noteworthy that the solid solutions may also interfere electrical transport, which makes the net increase in ZT values rely on the competition between the mobility loss and the reduction on κ_L.[94] Grain boundaries can scatter long-wavelength phonons which otherwise are hard to be interfered with by other mechanisms, i.e., $\tau_B^{-1} = v_g/L$(L is the grain size). For TE polycrystalline materials with micrometer grain sizes, grain boundary scattering dominates only at very low temperatures. However, the situation changes when the grain size is further reduced to nanoscale. We summarised some useful theoretical guidance for better quantification regarding nanostructures in 'From the conventional phonon–phonon interactions to nanostructures'.

PPIs, due to their rates increasing with the temperature, dominate the heat transport from room to high temperatures for the majority of TE materials. Slack has proposed a simple but useful model for high-temperature κ_L,[96]

$$\kappa_L = A \cdot \frac{\overline{m}\theta_D^3 \delta}{\gamma^2 N^{\frac{2}{3}} T}. \tag{15}$$

Here N is the number of atoms in the cell, δ^3 is the volume per atom, θ_D is the Debye temperature, and A is a γ-related parameter, respectively. Since the parameters can be approximately obtained from experiments, equation (15) is often used to give a qualitative description of the κ_L for simple TE compounds. The third-order IFC method in recent years has taken into account transitions among all possible combinations of three phonons and applies the Fermi's golden rule. Although these calculations are a textbook knowledge, the implementation of IFC calculations can provide a quantitative description of heat transport in most TE materials, as well as the choices of the nanostructure size ('From the conventional phonon–phonon interactions to nanostructures').

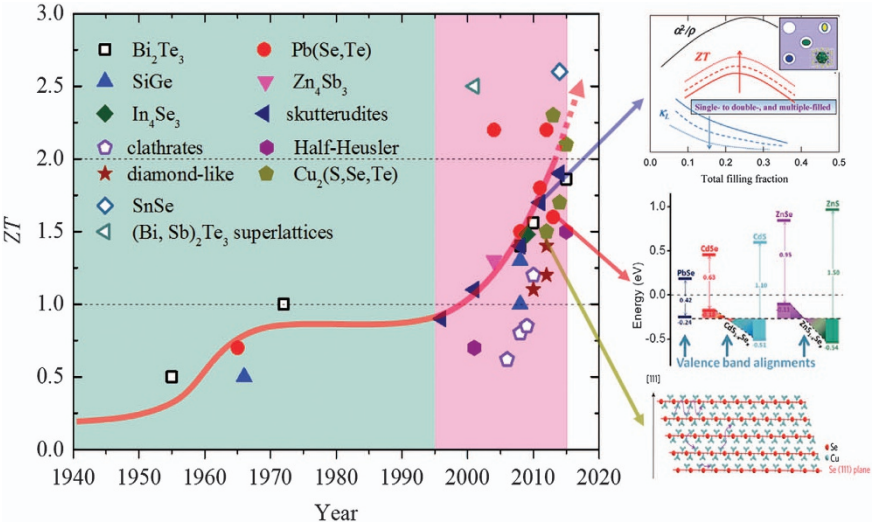

Figure 10. The chronological evolution of ZT values in various thermoelectric materials,[22,31,38,54,69,104,109,124,132,150,160–181] and the three detailed examples (PbSe matrix with band aligned nanocomposites,[31] *n*-type filled skutterudites,[69] and superionic compound Cu_2Se[150]).

In addition to the above discussed mechanisms, very recently, electron–phonon scattering was also found to limit κ_L. In Si, large amount of heat will be scattered if the carrier concentration is high due to a much enhanced electron–phonon interaction, as reported by Liao *et al.*[157] Considering that many TE materials have fairly high carrier concentrations (10^{20}–10^{21} cm^{-3}), the electron-phonon interaction is likely to be a player in reducing the κ_L. Experimentally, the noticeable influence of electron–phonon interaction has been pointed out in some heavily doped TE materials, such as SiGe[158] and Mo_3Se_7.[159]

When going beyond the conventional solids, the above mentioned small-perturbative methods have already become questionable or even invalid. The current implementation consists of introducing a phenomenological resonant scattering term as shown in equation (11) and treating it as another resistive scattering process. This is still done with well-defined phonons. A better description is necessary for providing the quantitative assessment in these systems. Possible solutions will depend on the extent of structural fluctuations. For compounds with modest fluctuations, such as the case with filled skutterudites, the temperature-dependent effective potential mentioned above might suffice. For compounds with structural fluctuations far beyond normal, statistical methods combined with classical and/or *ab initio* molecular dynamics simulations are possible ways with which to tackle the problem, including both the equilibrium molecular dynamics (based on the Green–Kubo formula), and the non-equilibrium molecular dynamics which traces the heat flux and temperature gradient.[151] Furthermore, the statistical methods can also be used to address and treat thermal transport processes on nano- or even mesoscales, which is useful for modelling of nanostructures.

SYNERGISTIC OPTIMISATION FOR HIGH ZTS

We have reviewed several different topics regarding both electrical and thermal transport processes so far. To achieve high ZT values in TE materials, a synergistic optimisation on both transport aspects is required. Armed with a deep understanding of transport phenomena, spectacular enhancements in the figure of merit ZT have been achieved in recent years across many families of TE materials,[22,31,38,54,69,104,109,124,132,150,160–181] as shown in Figure 10. Many traditional TE materials have doubled their ZT and new promising material systems have been identified and optimised. In this section, we will briefly summarise three different compounds with optimised power factors and low lattice thermal conductivities, including PbSe matrix with band-aligned nanostructures, *n*-type filled $CoSb_3$-based skutterudites, and the superionic material Cu_2Se and its sister compounds. There are, of course, other compounds with equally good or perhaps even better TE performance than the examples above. We have chosen materials that have not only a tremendous potential as thermoelectrics but also because they illustrate interesting physical phenomena and an excellent synergy between the theory and experimental efforts.

As mentioned, nanostructures in bulk TE materials reduce the κ_L by the interface scattering. In order to improve the *ZT* by incorporating nanostructures, it is essential to preserve or perhaps even enhance the electrical transport properties. Making an assumption that the mobility is mainly affected by the band edge offset between the matrix and inclusions in IV–VI rock-salt compounds, Zhao *et al.* proposed a 'minimal valence band offset' strategy[30,31,182] to minimise scattering of carriers at interfaces. The case demonstrating this idea was the matrix of PbSe composited with alloys of $CdS_{1-x}Se_x/ZnS_{1-x}Se_x$.[31] *Ab initio* calculations indicated that cadmium and zinc selenides have positive band offsets with respect to PbSe and the corresponding sulfides have negative offset values. Thus, the alloys of selenide and sulfide were used to get almost zero offset inclusions, and maintained the transport of electrons. Furthermore, by substituting Cd for Pb, the energy separation between L and Σ pockets decreased, and the Seebeck coefficient was thus enhanced. The two beneficial effects in the electrical transport, together with the much reduced κ_L by the nanostructure, resulted in the figure of merit $ZT \sim 1.6$ at 923 K (Figure 10), the highest value for tellurium-free chalcogenides. In a composite system, the use of band engineering to optimise the electronic properties is a worthwhile effort. Whether the concept of 'minimal band offset' is limited to IV–VI compounds or whether it will serve as a general guidance, however, requires further research efforts.

N-type partially filled skutterudites are among the first generation of 'new' compounds that have emerged from the era of 'big ideas' in the mid-1990s. After the initial exploratory efforts, the experimentalists found that large structural voids in the skutterudite lattice can be partially filled with certain rare earth and alkaline earth metals and both the electron concentration and the lattice thermal conductivity could be tuned. In 2005, Shi *et al.* concluded that the filling fraction limit in $CoSb_3$-based skutterudites is determined by the competition between the

filled phases and the secondary phases.[183] By calculating total energies of both phases, they not only reproduced the available experimental filling fraction limits at that time but also predicted new fillers among the alkaline metals and, in follow-up studies, pointed out the possibilities of multiple element filling.[66,184–186] As for the electrical transport, due to the large electronegativity difference between the guest and host species, the outermost *s* electrons of the filler atoms are donated to the conduction band of $CoSb_3$ without much band alteration.[67] Thus revealed rigidity of the band structure of filled $CoSb_3$-based skutterudites and the optimal doping levels make the carrier concentration tuning merely a simple electron counting exercise based on the charge state and the filling fraction of the fillers.[69] Power factors over 50 μW cm^{-1} K^{-2} can be easily obtained upon attaining the proper electron count (Figure 10). For the thermal transport, the resonant scattering mechanism has historically been used to describe variations in κ_L which is consistent with large displacements of the fillers. Theoretical determination of the resonant frequencies for a variety of fillers in 2007 was a milestone for the performance advance of filled $CoSb_3$ as it revealed the physical meaning of the previously merely fitting parameter.[131] Multiple filling was then proposed to scatter a broader range of phonons. Experimentally, by selecting rattling species such as Ba, La, Yb with frequencies of 93, 66, 42 cm^{-1}, respectively, the κ_L of such multiple filled $CoSb_3$-based skutterudites was gradually reduced from values corresponding to single, to double and to multiple filled structures.[69] Throughout the whole process one could witness a good integration of theoretical input and insights with experimental studies which enriched the understanding in this material system and resulted in enhanced values of ZT ~ 1.7 (Figure 10).[69]

In 2012, Liu *et al.* reported on the experimental work with Cu_2Se which had a ZT of 1.5 at 1,000 K, as shown in Figure 10.[150] This compound inherits features of the chemical bond hierarchy, namely a weakly bonded Cu ion sublattice and a rigid Se sublattice. However, the bonds between Cu and Se are so weak that they give rise to a liquid-like Cu movement in the high temperature antifluorite β phase. The ion fluidity is the unique aspect of Cu_2Se that immediately stimulated considerable research interest. The lattice thermal conductivities maintain their extremely low values (around 0.4–0.6 W m^{-1} K^{-1} in the entire temperature range). The quantification of the lattice dynamics, however, is difficult using the standard IFC calculations due to fast movements of Cu ions, which breaks down the perturbation assumptions, and static methods have to be considered as shown.[151] As a promising TE material, Cu_2Se shows a good electrical conductivity (10^4 ~ 10^5 S m^{-1}) and a large Seebeck coefficient (100 ~ 300 μV K^{-1}). The deficiency of Cu seems to be a good source of holes. There crystal-like electrical transport properties in Cu_2Se suggest a conductive network, though variations in electrical transport properties have not yet been rationalised. The sister compounds, Cu_2S and Cu_2Te, also demonstrate interesting properties such as even lower κ_L of Cu_2S[179], and a very complicated phase diagram of Cu_2Te.[187] The solid solutions of Cu_2S and Cu_2Te form nanoscale mosaic crystals with ZT values of up to 2.1 at 1,000 K.[180] Overall, copper chalcogenide compounds with their large ion mobility offer high TE performance as well as new physics and rich chemistry, representing a new research direction to explore for both experimentalists and theorists.

CONCLUDING REMARKS AND OUTLOOK

In this work, we have reviewed several topics pertaining to the high TE performance of TE materials. The viewpoint was mostly theoretical. Indeed, the theoretical insight has helped with the rationalisation of experimental approaches and speeded up the TE materials research in many aspects. Explicitly, band engineering has been widely adopted for studies of the electrical transport, including the band convergence, a reduction of the DOS to achieve weaker scattering of charge carriers, and the role of conductive networks in complex compounds. Interatomic force constant calculations, carried out in both harmonic and anharmonic approximations, can be used to advance understanding of the influence of nanostructures and of the PPI in conventional solids. Unconventional solids, such as those possessing phonon liquid features were also identified and studied both theoretically and experimentally. Because of advances in the theoretical understanding of transport phenomena, more powerful facilities combined with faster algorithms, and the integration of theory with experiment, TE research has evolved from a rather minor and sleepy field into an intense, worldwide and highly interdisciplinary activity, which gains from a unique perspective of physicists, chemists, engineers and computer modelers. The remaining challenges are the developments of methodologies for solving scattering problems and, specifically, problems concerning of carrier scatterings. Another challenge of the theoretical perspective is how to deal with transport in systems showing large atomic displacement parameters or even large structural fluctuations. Such structures encompass important families of TE materials and it is imperative to understand and predict their transport behaviour.

High throughput calculations are another area of considerable interest as it offers a timely and inexpensive identification of promising TE materials. The current standard is to screen potential compounds from a large compound library, usually a crystalline database, and then study them in detail with property descriptors. The screening for compounds with a lone-pair of electrons has been carried out in this way.[188] More high-throughput theoretical studies focus on half-Heusler alloys and related 1:1:1 compounds because of their simple unit cells and the large variety of elemental combinations. Yang *et al.* carried out electrical transport calculations under the CRTA to evaluate the power factor and the optimal doping level in 35 half-Heusler alloys.[189] Promising compounds are predicted and several of them are confirmed years later.[47,174] Anharmonic IFC calculations were used by Carrete *et al.* to evaluate the lattice thermal conductivity of 75 half-Heusler alloys out of 79,057 entries.[190] These results, combined with the electrical transport calculations, result to the ZT evaluations, with about 15 % of these compounds may have ZT > 2 at high temperatures.[191] In general, current high throughput studies are still in their infancy and offer only limited accuracy. It remains indispensable to carry out trial-and-error studies for the best proposed compositions. In this regard, more accurate descriptors are needed to nail down the right composition.[192] On the experimental side, very little work is done currently on high-throughput screening.[193] The culprit is the critical conditions necessary to follow when synthesising TE bulk materials. New techniques for rapid synthesis, such as the self-propagating high-temperature synthesis,[194] could be a solution to high-throughput experimentation with TE materials.

Finally, we note that it was not so long ago when the highest ZT known in any material was less than unity, and there were even researchers who held that ZT of unity could never be exceeded. Now there are several families of TE materials with ZT values approaching and even exceeding 2, a fact that has enormous implications for applications. This change has not come about by chance, but in fact is a consequence of applications of modern theory and complementary experimental efforts that exploit new understanding and ideas in the search for high performance TE materials. It may be that to achieve another big jump in the development of TE materials, however, new 'big ideas' as influential as was the PGEC paradigm and the concept of nanostructures some 20 years ago will be needed. Many of the topics reviewed above are closely connected to these original concepts. With the help of theory, new and exciting phenomena have been discovered that have helped shape the direction of TE

research. These include band convergence, scattering engineering, all-scale phonon scattering, minimum band offset for nanocomposites, partial crystalline-partial liquid compounds with structural fluctuations, to name a few. With the help of new 'big ideas' there is a good chance that novel structural forms of highly efficient TE materials would be discovered.

ACKNOWLEDGEMENTS

This work was supported by National Basic Research Program of China (973-program) under project number 2013CB632501, National Natural Science Foundation of China under contract number 11234012, the Key Research Program of Chinese Academy of Sciences (Grant No. KGZD-EW-T06), research grants (14DZ2261200 and 15JC1400301) from Science and Technology Commission of Shanghai Municipality, and International S&T Cooperation Program of China (2015DFA51050). Research of C. Uher was supported by the U.S. Department of Energy, Office of Basic Energy Sciences under award number DE-SC-0008574. Work at the University of Missouri (DJS) was supported by the Department of Energy through the S3TEC Energy Frontier Research Center award #DE-SC0001299/DE-FG02–09ER46577. Research of Jihui Yang was supported by the U.S. Department of Energy under corporate agreement DE-FC26-04NT42278, by GM, and by National Science Foundation under award number 1235535. WQ and LD also thank to the support from Shanghai Institute of Materials Genome.

COMPETING INTERESTS

The authors declare no conflict of interest.

REFERENCES

1. Goldsmid, H. J. *Introduction to Thermoelectricity* (Springer, 2010).
2. Ioffe, A. F. *Semiconductor thermoelements, and Thermoelectric cooling*, Reviewd and supplemented for the English edition. Translated from the Russian by A. Gelbtuch (Infosearch, 1957).
3. Snyder, G. J. & Toberer, E. S. Complex thermoelectric materials. *Nat. Mater.* **7**, 105–114 (2008).
4. Liu, W., Yan, X., Chen, G. & Ren, Z. Recent advances in thermoelectric nanocomposites. *Nano Energy* **1**, 42–56 (2012).
5. Hicks, L. & Dresselhaus, M. Effect of quantum-well structures on the thermoelectric figure of merit. *Phys. Rev. B* **47**, 12727 (1993).
6. Hicks, L. D., Harman, T. C., Sun, X. & Dresselhaus, M. S. Experimental study of the effect of quantum-well structures on the thermoelectric figure of merit. *Phys. Rev. B* **53**, 10493–10496 (1996).
7. Minnich, A. J., Dresselhaus, M. S., Ren, Z. F. & Chen, G. Bulk nanostructured thermoelectric materials: current research and future prospects. *Energy Environ. Sci.* **2**, 466–479 (2009).
8. Heremans, J. P., Dresselhaus, M. S., Bell, L. E. & Morelli, D. T. When thermoelectrics reached the nanoscale. *Nat. Nanotechnol.* **8**, 471–473 (2013).
9. Slack, G. A. in *CRC Handbook of Thermoelectrics* (ed Rowe D. M.) Ch. 9 (CRC Press, 1995).
10. Chen, Y. L. *et al.* Experimental realization of a three-dimensional topological insulator, Bi_2Te_3. *Science* **325**, 178–181 (2009).
11. May, A. F., Singh, D. J. & Snyder, G. J. Influence of band structure on the large thermoelectric performance of lanthanum telluride. *Phys. Rev. B* **79**, 153101 (2009).
12. Madsen, G. K. H. & Singh, D. J. BoltzTraP. A code for calculating band-structure dependent quantities. *Comput. Phys. Commun.* **175**, 67–71 (2006).
13. Pei, Y. Z., Wang, H. & Snyder, G. J. Band engineering of thermoelectric materials. *Adv. Mater.* **24**, 6125–6135 (2012).
14. Liu, W. *et al.* Convergence of conduction bands as a means of enhancing thermoelectric performance of n-Type Mg2Si1-xSnx solid solutions. *Phys. Rev. Lett.* **108**, 166601 (2012).
15. Bahk, J. H., Bian, Z. X. & Shakouri, A. Electron transport modeling and energy filtering for efficient thermoelectric Mg2Si1-xSnx solid solutions. *Phys. Rev. B* **89**, 075204 (2014).
16. Chen, S. Y., Gong, X. G., Walsh, A. & Wei, S. H. Electronic structure and stability of quaternary chalcogenide semiconductors derived from cation cross-substitution of II-VI and I-III-VI2 compounds. *Phys. Rev. B* **79**, 165211 (2009).
17. Zhang, J. W. *et al.* High-performance pseudocubic thermoelectric materials from non-cubic chalcopyrite compounds. *Adv. Mater.* **26**, 3848–3853 (2014).
18. Zeier, W. G. *et al.* Band convergence in the non-cubic chalcopyrite compounds Cu2MGeSe4. *J. Mater. Chem. C* **2**, 10189–10194 (2014).
19. Singh, D. J. Doping-dependent thermopower of PbTe from Boltzmann transport calculations. *Phys. Rev. B* **81**, 195217 (2010).
20. Chen, X., Parker, D. & Singh, D. J. Importance of non-parabolic band effects in the thermoelectric properties of semiconductors. *Sci. Rep.* **3**, 3168 (2013).
21. Tauber, R. N., Machonis, A. A. & Cadoff, I. B. Thermal and optical energy gaps in PbTe. *J. Appl. Phys.* **37**, 4855 (1966).
22. Pei, Y. Z. *et al.* Convergence of electronic bands for high performance bulk thermoelectrics. *Nature* **473**, 66–69 (2011).
23. Zhu, H., Sun, W. H., Armiento, R., Lazic, P. & Ceder, G. Band structure engineering through orbital interaction for enhanced thermoelectric power factor. *Appl. Phys. Lett.* **104**, 082107 (2014).
24. Skelton, J. M., Parker, S. C., Togo, A., Tanaka, I. & Walsh, A. Thermal physics of the lead chalcogenides PbS, PbSe, and PbTe from first principles. *Phys. Rev. B* **89**, 205203 (2014).
25. Kim, H. & Kaviany, M. Effect of thermal disorder on high figure of merit in PbTe. *Phys. Rev. B* **86**, 045213 (2012).
26. Gibbs, Z. M. *et al.* Temperature dependent band gap in PbX (X = S, Se, Te). *Appl. Phys. Lett.* **103**, 262109 (2013).
27. Wu, D. *et al.* Origin of the high performance in GeTe-based thermoelectric materials upon Bi2Te3 doping. *J. Am. Chem. Soc.* **136**, 11412–11419 (2014).
28. Pei, Y. Z., Wang, H., Gibbs, Z. M., LaLonde, A. D. & Snyder, G. J. Thermopower enhancement in Pb1-xMnxTe alloys and its effect on thermoelectric efficiency. *NPG Asia Mater.* **4**, e28 (2012).
29. Zhao, L. D. *et al.* All-scale hierarchical thermoelectrics: MgTe in PbTe facilitates valence band convergence and suppresses bipolar thermal transport for high performance. *Energy Environ. Sci.* **6**, 3346–3355 (2013).
30. Zhao, L. D., Dravid, V. P. & Kanatzidis, M. G. The panoscopic approach to high performance thermoelectrics. *Energy Environ. Sci.* **7**, 251–268 (2014).
31. Zhao, L. D. *et al.* High thermoelectric performance via hierarchical compositionally alloyed nanostructures. *J. Am. Chem. Soc.* **135**, 7364–7370 (2013).
32. Banik, A., Shenoy, U. S., Anand, S., Waghmare, U. V. & Biswas, K. Mg alloying in SnTe facilitates valence band convergence and optimizes thermoelectric properties. *Chem. Mater.* **27**, 581–587 (2015).
33. Lusakowski, A., Boguslawski, P. & Radzynski, T. Calculated electronic structure of Pb1-xMnxTe ($0 <= x < 11\%$): The role of L and Sigma valence band maxima. *Phys. Rev. B* **83**, 115206 (2011).
34. Tan, X. J., Shao, H. Z., Hu, T. Q., Liu, G. Q. & Ren, S. F. Theoretical understanding on band engineering of Mn-doped lead chalcogenides PbX (X = Te, Se, S). *J. Phys. Condens. Matter* **27**, 095501 (2015).
35. Heremans, J. P., Wiendlocha, B. & Chamoire, A. M. Resonant levels in bulk thermoelectric semiconductors. *Energy Environ. Sci* **5**, 5510–5530 (2012).
36. Wiendlocha, B. Fermi surface and electron dispersion of PbTe doped with resonant Tl impurity from KKR-CPA calculations. *Phys. Rev. B* **88**, 205205 (2013).
37. Tan, G. J. *et al.* Codoping in SnTe: enhancement of thermoelectric performance through synergy of resonance levels and band convergence. *J. Am. Chem. Soc.* **137**, 5100–5112 (2015).
38. Heremans, J. P. *et al.* Enhancement of thermoelectric efficiency in PbTe by distortion of the electronic density of states. *Science* **321**, 554–557 (2008).
39. Xiong, K. *et al.* Behaviour of group IIIA impurities in PbTe: implications to improve thermoelectric efficiency. *J. Phys. D Appl. Phys.* **43**, 405403 (2010).
40. Jaworski, C. M., Kulbachinskii, V. & Heremans, J. P. Resonant level formed by tin in Bi2Te3 and the enhancement of room-temperature thermoelectric power. *Phys. Rev. B* **80**, 233201 (2009).
41. Lan, J. L. *et al.* Enhanced Thermoelectric Properties of Pb-doped BiCuSeO Ceramics. *Adv. Mater.* **25**, 5086–5090 (2013).
42. Cui, J. L., Li, Y. P., Du, Z. L., Meng, Q. S. & Zhou, H. Promising defect thermoelectric semiconductors Cu1-xGaSbxTe2 (x = 0-0.1) with the chalcopyrite structure. *J. Mater. Chem. A* **1**, 677–683 (2013).
43. Qiu, P. F., Yang, J., Huang, X. Y., Chen, X. H. & Chen, L. D. Effect of antisite defects on band structure and thermoelectric performance of ZrNiSn half-Heusler alloys. *Appl. Phys. Lett.* **96**, 152105 (2010).
44. Wu, L. *et al.* Two-dimensional thermoelectrics with Rashba spin-split bands in bulk BiTeI. *Phys. Rev. B* **90**, 202115 (2014).
45. Putley, E. H. *The Hall Effect And Related Phenomena* (Butterworths, 1960).
46. Yang, J. *et al.* Power factor enhancement in light valence band p-type skutterudites. *Appl. Phys. Lett.* **101**, 022101 (2012).
47. Fu, C. G., Zhu, T. J., Liu, Y. T., Xie, H. H. & Zhao, X. B. Band engineering of high performance p-type FeNbSb based half-Heusler thermoelectric materials for figure of merit $zT > 1$. *Energy Environ. Sci.* **8**, 216–220 (2015).
48. Pei, Y. Z., LaLonde, A. D., Wang, H. & Snyder, G. J. Low effective mass leading to high thermoelectric performance. *Energy Environ. Sci.* **5**, 7963–7969 (2012).
49. Lee, D. S. *et al.* Density of state effective mass and related charge transport properties in K-doped BiCuOSe. *Appl. Phys. Lett.* **103**, 232110 (2013).
50. Dyck, J. S. *et al.* Thermoelectric properties of the n-type filled skutterudite Ba0.3Co4Sb12 doped with Ni. *J. Appl. Phys.* **91**, 3698–3705 (2002).

51. Dyck, J. S., Chen, W., Yang, J. H., Meisner, G. P. & Uher, C. Effect of Ni on the transport and magnetic properties of Co1-xNixSb3. *Phys. Rev. B* **65**, 115204 (2002).
52. Li, X. Y. *et al.* Thermoelectric properties of Te-doped CoSb3 by spark plasma sintering. *J. Appl. Phys.* **98**, 083702 (2005).
53. Wang, S. *et al.* On intensifying carrier impurity scattering to enhance thermoelectric performance in Cr-doped CeyCo4Sb12. *Adv. Funct. Mater.* **25**, 6660–6670 (2015).
54. Shi, X. *et al.* On the design of high-efficiency thermoelectric clathrates through a systematic cross-substitution of framework elements. *Adv. Funct. Mater.* **20**, 755–763 (2010).
55. Suh, J. *et al.* Simultaneous enhancement of electrical conductivity and thermopower of Bi2Te3 by multifunctionality of native defects. *Adv. Mater.* **27**, 3681–3686 (2015).
56. Faleev, S. V. & Leonard, F. Theory of enhancement of thermoelectric properties of materials with nanoinclusions. *Phys. Rev. B* **77**, 214304 (2008).
57. Martin, J., Wang, L., Chen, L. & Nolas, G. S. Enhanced Seebeck coefficient through energy-barrier scattering in PbTe nanocomposites. *Phys. Rev. B* **79**, 115311 (2009).
58. Zeng, G. H. *et al.* Cross-plane Seebeck coefficient of ErAs: InGaAs/InGaAlAs superlattices. *J. Appl. Phys.* **101**, 034502 (2007).
59. Shakouri, A. Recent developments in semiconductor thermoelectric physics and materials. *Annu. Rev. Mater. Res.* **41**, 399–431 (2011).
60. Makongo, J. P. A. *et al.* Simultaneous large enhancements in thermopower and electrical conductivity of bulk nanostructured half-heusler alloys. *J. Am. Chem. Soc.* **133**, 18843–18852 (2011).
61. Liu, Y. *et al.* Large enhancements of thermopower and carrier mobility in quantum dot engineered bulk semiconductors. *J. Am. Chem. Soc.* **135**, 7486–7495 (2013).
62. Yu, B. *et al.* Enhancement of thermoelectric properties by modulation-doping in silicon germanium alloy nanocomposites. *Nano Lett.* **12**, 2077–2082 (2012).
63. Xu, Y., Gan, Z. X. & Zhang, S. C. Enhanced thermoelectric performance and anomalous Seebeck effects in topological insulators. *Phys. Rev. Lett.* **112**, 226801 (2014).
64. Shi, H., Parker, D., Du, M.-H. & Singh, D. J. Connecting thermoelectric performance and topological-insulator behavior: Bi_2Te_3 and Bi_2Te_2Se from first principles. *Phys. Rev. Appl.* **3**, 014004 (2015).
65. Sofo, J. O. & Mahan, G. D. Electronic structure of $CoSb_3$: a narrow-band-gap semiconductor. *Phys. Rev. B* **58**, 15620–15623 (1998).
66. Mei, Z. G., Yang, J., Pei, Y. Z., Zhang, W. & Chen, L. D. Alkali-metal-filled $CoSb_3$ skutterudites as thermoelectric materials: theoretical study. *Phys. Rev. B* **77**, 045202 (2008).
67. Yang, J., Xi, L., Zhang, W., Chen, L. D. & Yang, J. Electrical transport properties of filled CoSb3 skutterudites: a theoretical study. *J. Electron. Mater.* **38**, 1397–1401 (2009).
68. Bai, S. Q. *et al.* Enhanced thermoelectric performance of dual-element-filled skutterudites BaxCeyCo4Sb12. *Acta Mater.* **57**, 3135–3139 (2009).
69. Shi, X. *et al.* Multiple-filled skutterudites: high thermoelectric figure of merit through separately optimizing electrical and thermal transports. *J. Am. Chem. Soc.* **133**, 7837–7846 (2011).
70. Yang, J. *et al.* Trends in electrical transport of p-type skutterudites RFe4Sb12 (R = Na, K, Ca, Sr, Ba, La, Ce, Pr, Yb) from first-principles calculations and Boltzmann transport theory. *Phys. Rev. B* **84**, 235205 (2011).
71. Xi, L. *et al.* Chemical bonding, conductive network, and thermoelectric performance of the ternary semiconductors Cu2SnX3 (X = Se, S) from first principles. *Phys. Rev. B* **86**, 155201 (2012).
72. Shi, X., Xi, L., Fan, J., Zhang, W. & Chen, L. Cu-Se bond network and thermoelectric compounds with complex diamondlike structure. *Chem. Mater.* **22**, 6029–6031 (2010).
73. Li, W. *et al.* Cu2HgSnSe4 nanoparticles: synthesis and thermoelectric properties. *CrystEngComm* **15**, 8966–8971 (2013).
74. Wang, B. *et al.* Heterovalent Substitution to Enrich Electrical Conductivity in Cu2CdSn1-xGaxSe4 Series for High Thermoelectric Performances. *Sci. Rep.* **5**, 9365 (2015).
75. Aydemir, U. *et al.* Thermoelectric enhancement in BaGa2Sb2 by Zn doping. *Chem. Mater.* **27**, 1622–1630 (2015).
76. He, H., Stearrett, R., Nowak, E. R. & Bobev, S. BaGa2Pn2 (Pn = P, As): new semiconducting phosphides and arsenides with layered structures. *Inorgan. Chem.* **49**, 7935–7940 (2010).
77. Toberer, E. S., May, A. F., Melot, B. C., Flage-Larsen, E. & Snyder, G. J. Electronic structure and transport in thermoelectric compounds AZn(2)Sb(2) (A = Sr, Ca, Yb, Eu). *Dalton Trans.* **39**, 1046–1054 (2010).
78. Wang, X.-J. *et al.* Synthesis and high thermoelectric efficiency of Zintl phase YbCd2-xZnxSb2. *Appl. Phys. Lett.* **94**, 092106 (2009).
79. Tandon, N., Albrecht, J. D. & Ram-Mohan, L. R. Electron-phonon coupling and associated scattering rates in diamond. *Diamond Relat. Mater.* **56**, 1–5 (2015).
80. Liao, B., Zhou, J., Qiu, B., Dresselhaus, M. S. & Chen, G. Ab initio study of electron-phonon interaction in phosphorene. *Phys. Rev. B* **91**, 235419 (2015).
81. Heremans, J. P., Thrush, C. M. & Morelli, D. T. Thermopower enhancement in lead telluride nanostructures. *Phys. Rev. B* **70**, 115334 (2004).
82. Sun, P. J. *et al.* Large Seebeck effect by charge-mobility engineering. *Nat. Commun.* **6**, 7475 (2015).
83. Abeles, B. Thermal conductivity of germanium in the temperature range 300°-1080 °K. *J. Phys. Chem. Solids* **8**, 340–343 (1959).
84. Kettel, F. Die Wärmeleitfähigkeit von Germanium bei hohen temperaturen. *J. Phys. Chem. Solids* **10**, 52–58 (1959).
85. Wang, S. *et al.* Conductivity-limiting bipolar thermal conductivity in semiconductors. *Sci. Rep.* **5**, 10136 (2015).
86. Ziman, J. M. *Electrons and Phonons; The Theory of Transport Phenomena in Solids* (Clarendon Press, 1960).
87. Yang, J. in *Thermal Conductivity: Theory, Properties and Applications*, edTritt T. M. Ch. 1.1, 1–20 (Kluwer Academic/Plenum Publishers, 2004).
88. Toberer, E. S., Zevalkink, A. & Snyder, G. J. Phonon engineering through crystal chemistry. *J. Mater. Chem.* **21**, 15843–15852 (2011).
89. Nolas, G. S., Sharp, J. & Goldsmid, H. J. *Thermoelectrics: Basic Principles and New Materials Developments* (Springer, 2001).
90. Hu, L. P., Zhu, T. J., Liu, X. H. & Zhao, X. B. Point defect engineering of high-performance bismuth-telluride-based thermoelectric materials. *Adv. Funct. Mater.* **24**, 5211–5218 (2014).
91. Petersen, A., Bhattacharya, S., Tritt, T. M. & Poon, S. J. Critical analysis of lattice thermal conductivity of half-Heusler alloys using variations of Callaway model. *J. Appl. Phys.* **117**, 035706 (2015).
92. Yang, J., Meisner, G. P. & Chen, L. Strain field fluctuation effects on lattice thermal conductivity of ZrNiSn-based thermoelectric compounds. *Appl. Phys. Lett.* **85**, 1140–1142 (2004).
93. Yan, X. *et al.* Stronger phonon scattering by larger differences in atomic mass and size in p-type half-Heuslers Hf1-xTixCoSb0.8Sn0.2. *Energy Environ. Sci.* **5**, 7543–7548 (2012).
94. Wang, H., LaLonde, A. D., Pei, Y. Z. & Snyder, G. J. The criteria for beneficial disorder in thermoelectric solid solutions. *Adv. Funct. Mater.* **23**, 1586–1596 (2013).
95. Wang, H., Wang, J. L., Cao, X. L. & Snyder, G. J. Thermoelectric alloys between PbSe and PbS with effective thermal conductivity reduction and high figure of merit. *J. Mater. Chem. A* **2**, 3169–3174 (2014).
96. Morelli, D. T., Slack, G. A. in *High Thermal Conductivity Materials* (eds Shindé S. L. & Goela J. S.) Ch. 2, 37–68 (Springer, 2006).
97. Lindsay, L., Broido, D. A. & Reinecke, T. L. Ab initio thermal transport in compound semiconductors. *Phys. Rev. B* **87**, 165201 (2013).
98. An, J. M., Subedi, A. & Singh, D. J. Ab initio phonon dispersions for PbTe. *Solid State Commun.* **148**, 417–419 (2008).
99. Zhang, Y., Ke, X. Z., Chen, C. F., Yang, J. & Kent, P. R. C. Thermodynamic properties of PbTe, PbSe, and PbS: First-principles study. *Phys. Rev. B* **80**, 024304 (2009).
100. Zhang, Y., Ke, X., Kent, P. R. C., Yang, J. & Chen, C. Anomalous lattice dynamics near the ferroelectric instability in PbTe. *Phys. Rev. Lett.* **107**, 175503 (2011).
101. Tian, Z. *et al.* Phonon conduction in PbSe, PbTe, and PbTe1-xSex from first-principles calculations. *Phys. Rev. B* **85**, 184303 (2012).
102. Lee, S. *et al.* Resonant bonding leads to low lattice thermal conductivity. *Nat. Commun.* **5**, 4525 (2014).
103. Li, C. *et al.* Orbitally driven giant phonon anharmonicity in SnSe. *Nat. Phys.* **11**, 1063 (2015).
104. Zhao, L. D. *et al.* Ultralow thermal conductivity and high thermoelectric figure of merit in SnSe crystals. *Nature* **508**, 373–377 (2014).
105. Carrete, J., Mingo, N. & Curtarolo, S. Low thermal conductivity and triaxial phononic anisotropy of SnSe. *Appl. Phys. Lett.* **105**, 101907 (2014).
106. Romero, A. H., Gross, E. K. U., Verstraete, M. J. & Hellman, O. Thermal conductivity in PbTe from first principles. *Phys. Rev. B* **91**, 214310 (2015).
107. Li, C. W. *et al.* Phonon self-energy and origin of anomalous neutron scattering spectra in SnTe and PbTe thermoelectrics. *Phys. Rev. Lett.* **112**, 175501 (2014).
108. Hellman, O. & Broido, D. A. Phonon thermal transport in Bi2Te3 from first principles. *Phys. Rev. B* **90**, 134309 (2014).
109. Biswas, K. *et al.* High-performance bulk thermoelectrics with all-scale hierarchical architectures. *Nature* **489**, 414–418 (2012).
110. Yang, J., Yip, H.-L. & Jen, A. K. Y. Rational design of advanced thermoelectric materials. *Adv. Energy Mater.* **3**, 565 (2013).
111. Guo, R., Wang, X. & Huang, B. Thermal conductivity of skutterudite CoSb3 from first principles: substitution and nanoengineering effects. *Sci. Rep.* **5**, 7806 (2015).
112. Katcho, N. A., Mingo, N. & Broido, D. A. Lattice thermal conductivity of (Bi1-xSbx)(2)Te-3 alloys with embedded nanoparticles. *Phys. Rev. B* **85**, 115208 (2012).

113. Yang, R. G. & Chen, G. Thermal conductivity modeling of periodic two-dimensional nanocomposites. *Phys. Rev. B* **69**, 195316 (2004).
114. Yang, R. G., Chen, G. & Dresselhaus, M. S. Thermal conductivity of simple and tubular nanowire composites in the longitudinal direction. *Phys. Rev. B* **72**, 125418 (2005).
115. Jeng, M. S., Yang, R. G., Song, D. & Chen, G. Modeling the thermal conductivity and phonon transport in nanoparticle composites using Monte Carlo simulation. *J. Heat Transfer* **130**, 042410 (2008).
116. Mingo, N., Hauser, D., Kobayashi, N. P., Plissonnier, M. & Shakouri, A. 'Nanoparticle-in-Alloy' Approach to Efficient Thermoelectrics: Silicides in SiGe. *Nano Lett.* **9**, 711–715 (2009).
117. Garg, J. & Chen, G. Minimum thermal conductivity in superlattices: A first-principles formalism. *Phys. Rev. B* **87**, 140302(R) (2013).
118. Zhang, H. & Minnich, A. J. The best nanoparticle size distribution for minimum thermal conductivity. *Sci. Rep.* **5**, 8995 (2015).
119. Chan, M. K. Y. *et al.* Cluster expansion and optimization of thermal conductivity in SiGe nanowires. *Phys. Rev. B* **81**, 174303 (2010).
120. Minnich, A. J. *et al.* Modeling study of thermoelectric SiGe nanocomposites. *Phys. Rev. B* **80**, 155327 (2009).
121. Wei, J. *et al.* Theoretical study of the thermoelectric properties of SiGe nanotubes. *RSC Adv.* **4**, 53037–53043 (2014).
122. Fiedler, G. & Kratzer, P. Theoretical prediction of improved figure-of-merit in Si/Ge quantum dot superlattices. *New J. Phys.* **15**, 125010 (2013).
123. Jeitschko, W. & Braun, D. LaFe4P12 with filled CoAs3-type structure and isotypic lanthanoid-transition metal polyphosphides. *Acta Crystallographica Section B* **33**, 3401–3406 (1977).
124. Sales, B. C., Mandrus, D. & Williams, R. K. Filled skutterudite antimonides: A new class of thermoelectric materials. *Science* **272**, 1325–1328 (1996).
125. Sales, B. C., Mandrus, D., Chakoumakos, B. C., Keppens, V. & Thompson, J. R. Filled skutterudite antimonides: Electron crystals and phonon glasses. *Phys. Rev. B* **56**, 15081–15089 (1997).
126. Chen, B. X. *et al.* Low-temperature transport properties of the filled skutterudites CeFe4-xCoxSb12. *Phys. Rev. B* **55**, 1476–1480 (1997).
127. Nolas, G. S., Cohn, J. L. & Slack, G. A. Effect of partial void filling on the lattice thermal conductivity of skudderudites. *Phys. Rev. B* **58**, 164–170 (1998).
128. Pohl, R. O. Thermal Conductivity and Phonon Resonance Scattering. *Phys. Rev. Lett.* **8**, 481 (1962).
129. Puyet, M. *et al.* Low-temperature thermal properties of n-type partially filled calcium skutterudites. *J. Phys. Condens. Matter* **18**, 11301–11308 (2006).
130. Yang, J. *et al.* Effect of Sn substituting for Sb on the low-temperature transport properties of ytterbium-filled skutterudites. *Phys. Rev. B* **67**, 165207 (2003).
131. Yang, J., Zhang, W., Bai, S. Q., Mei, Z. & Chen, L. D. Dual-frequency resonant phonon scattering in BaxRyCo4Sb12 (R = La, Ce, and Sr). *Appl. Phys. Lett.* **90**, 192111 (2007).
132. Shi, X. *et al.* Low thermal conductivity and high thermoelectric figure of merit in n-type $Ba_xYb_yCo_4Sb_{12}$ double-filled skutterudites. *Appl. Phys. Lett.* **92**, 182101 (2008).
133. Bai, S. Q., Shi, X. & Chen, L. D. Lattice thermal transport in BaxREyCo4Sb12 (RE = Ce, Yb, and Eu) double-filled skutterudites. *Appl. Phys. Lett.* **96**, 202102 (2010).
134. Liu, R. *et al.* p-Type skutterudites RxMyFe3CoSb12 (R, M = Ba, Ce, Nd, and Yb): Effectiveness of double-filling for the lattice thermal conductivity reduction. *Intermetallics* **19**, 1747–1751 (2011).
135. Koza, M. M. *et al.* Breakdown of phonon glass paradigm in La- and Ce-filled Fe(4) Sb(12) skutterudites. *Nat. Mater.* **7**, 805–810 (2008).
136. Christensen, M. *et al.* Avoided crossing of rattler modes in thermoelectric materials. *Nat. Mater.* **7**, 811–815 (2008).
137. Zebarjadi, M., Esfarjani, K., Yang, J. A., Ren, Z. F. & Chen, G. Effect of filler mass and binding on thermal conductivity of fully filled skutterudites. *Phys. Rev. B* **82**, 195207 (2010).
138. Koza, M. M. *et al.* Low-energy phonon dispersion in LaFe4Sb12. *Phys. Rev. B* **91**, 014305 (2015).
139. Thompson, D. R. *et al.* Rare-earth free p-type filled skutterudites: Mechanisms for low thermal conductivity and effects of Fe/Co ratio on the band structure and charge transport. *Acta Mater.* **92**, 152–162 (2015).
140. Li, W. & Mingo, N. Thermal conductivity of fully filled skutterudites: Role of the filler. *Phys. Rev. B* **89**, 184304 (2014).
141. Li, W. & Mingo, N. Ultralow lattice thermal conductivity of the fully filled skutterudite YbFe4Sb12 due to the flat avoided-crossing filler modes. *Phys. Rev. B* **91**, 144304 (2015).
142. Avila, M. A. *et al.* Ba(8)Ga(16)Sn(30) with type-I clathrate structure: Drastic suppression of heat conduction. *Appl. Phys. Lett.* **92**, 041901 (2008).
143. Takabatake, T., Suekuni, K. & Nakayama, T. Phonon-glass electron-crystal thermoelectric clathrates: Experiments and theory. *Reviews of Modern Physics* **86**, 669–716 (2014).
144. Nakayama, T. & Kaneshita, E. Significance of Off-Center Rattling for Emerging Low-Lying THz Modes in Type-I Clathrates. *Journal of the Physical Society of Japan* **80**, 104604 (2011).
145. Voneshen, D. J. *et al.* Suppression of thermal conductivity by rattling modes in thermoelectric sodium cobaltate. *Nat. Mater.* **12**, 1027–1031 (2013).
146. Qiu, W., Wu, L., Ke, X., Yang, J. & Zhang, W. Diverse lattice dynamics in ternary Cu-Sb-Se compounds. *Sci. Rep.* **5**, 13643 (2015).
147. Qiu, W. J. *et al.* Part-crystalline part-liquid state and rattling-like thermal damping in materials with chemical-bond hierarchy. *Proceedings of the National Academy of Sciences of the United States of America* **111**, 15031–15035 (2014).
148. Skoug, E. J. & Morelli, D. T. Role of Lone-Pair Electrons in Producing Minimum Thermal Conductivity in Nitrogen-Group Chalcogenide Compounds. *Phys. Rev. Lett.* **107**, 235901 (2011).
149. Zhang, Y. S. *et al.* First-principles description of anomalously low lattice thermal conductivity in thermoelectric Cu-Sb-Se ternary semiconductors. *Phys. Rev. B* **85**, 054306 (2012).
150. Liu, H. L. *et al.* Copper ion liquid-like thermoelectrics. *Nat. Mater.* **11**, 422–425 (2012).
151. Kim, H. *et al.* Ultralow thermal conductivity of b-Cu2Se by atomic fluidity and structure distortion. *Acta Mater.* **86**, 247–253 (2015).
152. Dennler, G. *et al.* Are binary copper sulfides/selenides really new and promising thermoelectric materials? *Adv. Energy Mater.* **4**, 1301581 (2014).
153. Callaway, J. Model for Lattice Thermal Conductivity at Low Temperatures. *Physical Review* **113**, 1046–1051 (1959).
154. Asen-Palmer, M. *et al.* Thermal conductivity of germanium crystals with different isotopic compositions. *Phys. Rev. B* **56**, 9431–9447 (1997).
155. Morelli, D. T., Heremans, J. P. & Slack, G. A. Estimation of the isotope effect on the lattice thermal conductivity of group IV and group III-V semiconductors. *Phys. Rev. B* **66**, 195304 (2002).
156. Ward, A., Broido, D. A., Stewart, D. A. & Deinzer, G. Ab initio theory of the lattice thermal conductivity in diamond. *Phys. Rev. B* **80**, 754 (2009).
157. Liao, B. L. *et al.* Significant reduction of lattice thermal conductivity by the electron-phonon interaction in silicon with high carrier concentrations: a first-principles study. *Phys. Rev. Lett.* **114**, 115901 (2015).
158. Vining, C. B. A model for the high-temperature transport-properties of heavily doped n-type silicon-germanium alloys. *J. Appl. Phys.* **69**, 331–341 (1991).
159. Shi, X., Pei, Y., Snyder, G. J. & Chen, L. Optimized thermoelectric properties of $Mo_3Sb_{7-x}Te_x$ with significant phonon scattering by electrons. *Energy Environ. Sci.* **4**, 4086–4095 (2011).
160. Poudel, B. *et al.* High-thermoelectric performance of nanostructured bismuth antimony telluride bulk alloys. *Science* **320**, 634–638 (2008).
161. Xie, W. *et al.* Identifying the specific nanostructures responsible for the high thermoelectric performance of $(Bi, Sb)_2Te_3$ nanocomposites. *Nano Lett.* **10**, 3283–3289 (2010).
162. Kim, S. I. *et al.* Dense dislocation arrays embedded in grain boundaries for high-performance bulk thermoelectrics. *Science* **348**, 109–114 (2015).
163. Hsu, K. F. *et al.* Cubic $AgPb_mSbTe_{2+m}$: Bulk thermoelectric materials with high figure of merit. *Science* **303**, 818–821 (2004).
164. Joshi, G. *et al.* Enhanced thermoelectric figure-of-merit in nanostructured p-type silicon germanium bulk alloys. *Nano Lett.* **8**, 4670–4674 (2008).
165. Wang, X. *et al.* Enhanced thermoelectric figure of merit in nanostructured n-type silicon germanium bulk alloy. *Appl. Phys. Lett.* **93**, 193121 (2008).
166. Snyder, G. J., Christensen, M., Nishibori, E., Caillat, T. & Iversen, B. B. Disordered zinc in Zn_4Sb_3 with phonon-glass and electron-crystal thermoelectric properties. *Nat. Mater.* **3**, 458–463 (2004).
167. Rhyee, J.-S. *et al.* Peierls distortion as a route to high thermoelectric performance in In4Se3-delta crystals. *Nature* **459**, 965–968 (2009).
168. Chen, L. *et al.* Anomalous barium filling fraction and *n*-type thermoelectric performance of $Ba_yCo_4Sb_{12}$. *J. Appl. Phys.* **90**, 1864 (2001).
169. Rogl, G. *et al.* n-Type skutterudites (R, Ba, Yb)yCo4Sb12 (R = Sr, La, Mm, DD, SrMm, SrDD) approaching ZT≈2.0. *Acta Mater.* **63**, 30–43 (2014).
170. Martin, J., Wang, H. & Nolas, G. S. Optimization of the thermoelectric properties of $Ba_8Ga_{16}Ge_{30}$. *Appl. Phys. Lett.* **92**, 222110 (2008).
171. Wang, L., Chen, L.-D., Chen, X.-H. & Zhang, W.-B. Synthesis and thermoelectric properties of n-type Sr8Ga16-xGe30-y clathrates with different Ga/Ge ratios. *J. Phys. Appl. Phys.* **42**, 045113 (2009).
172. Fujita, I., Kishimoto, K., Sato, M., Anno, H. & Koyanagi, T. Thermoelectric properties of sintered clathrate compounds $Sr_8Ga_xGe_{46-x}$ with various carrier concentrations. *J. Appl. Phys.* **99**, 093707 (2006).
173. Shen, Q. *et al.* Effects of partial substitution of Ni by Pd on the thermoelectric properties of ZrNiSn-based half-Heusler compounds. *Appl. Phys. Lett.* **79**, 4165–4167 (2001).
174. Fu, C. *et al.* Realizing high figure of merit in heavy-band p-type half-Heusler thermoelectric materials. *Nat. Commun.* **6**, 8144 (2015).

175. Shi, X. Y., Xi, L. L., Fan, J., Zhang, W. Q. & Chen, L. D. Cu-Se bond network and thermoelectric compounds with complex diamondlike structure. *Chem. Mater.* **22**, 6029–6031 (2010).
176. Liu, R. *et al.* Ternary compound $CuInTe_2$: a promising thermoelectric material with diamond-like structure. *Chemical Communications* **48**, 3818–3820 (2012).
177. Plirdpring, T. *et al.* Chalcopyrite CuGaTe2: A High-Efficiency Bulk Thermoelectric Material. *Adv. Mater.* **24**, 3622–3626 (2012).
178. Liu, H. L. *et al.* Ultrahigh thermoelectric performance by electron and phonon critical scattering in Cu2Se1-xIx. *Adv. Mater.* **25**, 6607–6612 (2013).
179. He, Y. *et al.* High thermoelectric performance in non-toxic earth-abundant copper sulfide. *Adv. Mater.* **26**, 3974–3978 (2014).
180. He, Y. *et al.* Ultrahigh thermoelectric performance in mosaic crystals. *Adv. Mater.* **27**, 3639–3644 (2015).
181. Venkatasubramanian, R., Siivola, E., Colpitts, T. & O'quinn, B. Thin-film thermoelectric devices with high room-temperature figures of merit. *Nature* **413**, 597–602 (2001).
182. Biswas, K. *et al.* Strained endotaxial nanostructures with high thermoelectric figure of merit. *Nat. Chem.* **3**, 160–166 (2011).
183. Shi, X., Zhang, W., Chen, L. D. & Yang, J. Filling fraction limit for intrinsic voids in crystals: Doping in skutterudites. *Phys. Rev. Lett.* **95**, 185503 (2005).
184. Xi, L., Yang, J., Zhang, W., Chen, L. & Yang, J. Anomalous dual-element filling in partially filled skutterudites. *J. Am. Chem. Soc.* **131**, 5560–5563 (2009).
185. Xi, L. *et al.* Systematic study of the multiple-element filling in caged skutterudite CoSb3. *Chem. Mater.* **22**, 2384–2394 (2010).
186. Zhang, W. *et al.* Predication of an ultrahigh filling fraction for K in CoSb3. *Appl. Phys. Lett.* **89**, 112105 (2006).
187. He, Y., Zhang, T., Shi, X., Wei, S.-H. & Chen, L. High thermoelectric performance in copper telluride. *NPG Asia Mater.* **7**, e210 (2015).
188. Nielsen, M. D., Ozolins, V. & Heremans, J. P. Lone pair electrons minimize lattice thermal conductivity. *Energy Environ. Sci.* **6**, 570–578 (2013).
189. Yang, J. *et al.* Evaluation of half-heusler compounds as thermoelectric materials based on the calculated electrical transport properties. *Adv. Funct. Mater.* **18**, 2880–2888 (2008).
190. Carrete, J., Li, W., Mingo, N., Wang, S. & Curtarolo, S. Finding unprecedentedly low-thermal-conductivity half-Heusler semiconductors via high-throughput materials modeling. *Phys. Rev. X* **4**, 011019 (2014).
191. Carrete, J., Mingo, N., Wang, S. & Curtarolo, S. Nanograined half-Heusler semiconductors as advanced thermoelectrics: an ab initio high-throughput statistical study. *Adv. Funct. Mater.* **24**, 7427–7432 (2014).
192. Yan, J. *et al.* Material descriptors for predicting thermoelectric performance. *Energy Environ. Sci.* **8**, 983–994 (2015).
193. Funahashi, R. *et al.* High-throughput screening of thermoelectric oxides and power generation modules consisting of oxide unicouples. *Meas Sci Technol* **16**, 70–80 (2005).
194. Su, X. L. *et al.* Self-propagating high-temperature synthesis for compound thermoelectrics and new criterion for combustion processing. *Nat. Commun.* **5**, 4908 (2014).